AFFDL-TR-75-121

F_G

SPECTRAL GUST RESPONSE FOR AN AIRPLANE WITH VERTICAL MOTION AND PITCH

ADA021713

AERONAUTICAL RESEARCH ASSOCIATES OF PRINCETON, INC.
50 WASHINGTON ROAD, PRINCETON, NEW JERSEY 08540

OCTOBER 1975

D D C

MAR 15 1976

D

AIR FORCE FLIGHT DYNAMICS LABORATORY
AIR FORCE WRIGHT AERONAUTICAL LABORATORIES
Air Force Systems Command
Wright-Patterson AFB, Ohio 45433

NOTICE

When Government drawings, specifications, or other data are used for any purpose other than in connection with a definitely related Government procurement operation, the United States Government thereby incurs no responsibility nor any obligation whatsoever; and the fact that the government may have formulated, furnished, or in any way supplied the said drawings, specifications, or other data, is not to be regarded by implication or otherwise as in any manner licensing the holder or any other person or corporation, or conveying any rights or permission to manufacture, use, or sell any patented invention that may in any way be related thereto.

This report has been reviewed by the Office of Information (OI) and is releasable to the National Technical Information Service (NTIS). At NTIS, it will be available to the general public, including foreign nations.

This technical report has been reviewed and is approved for publication.

ROBERT M. BADER, Chief
Structural Integrity Branch
Structures Division
AF Flight Dynamics Laboratory

PAUL L. HASTY
Project Engineer

FOR THE COMMANDER

GERALD G. LEIGH, Lt. Col., USAF
Chief, Structures Division

Copies of this report should not be returned unless return is required by security considerations, contractual obligations, or notice on a specific document.

Final Technical rept.
1 Nov 74 - 30 Sep 75,

UNCLASSIFIED
SECURITY CLASSIFICATION OF THIS PAGE (When Data Entered)

REPORT DOCUMENTATION PAGE		READ INSTRUCTIONS BEFORE COMPLETING FORM
1. REPORT NUMBER AFFDL-TR-75-121	2. GOVT ACCESSION NO.	3. RECIPIENT'S CATALOG NUMBER
4. TITLE (and Subtitle) SPECTRAL GUST RESPONSE FOR AN AIRPLANE WITH VERTICAL MOTION AND PITCH		5. TYPE OF REPORT & PERIOD COVERED Final 11/1/74-9/30/75
		6. PERFORMING ORG. REPORT NUMBER A.R.A.P. 256
7. AUTHOR(s) John C. Houbolt & Guy G. Williamson		8. CONTRACT OR GRANT NUMBER(s) F33615-75-C-3030 NEW
8. PERFORMING ORGANIZATION NAME AND ADDRESS Aeronautical Research Associates of Princeton, Inc., 50 Washington Road, Princeton, New Jersey 08540		10. PROGRAM ELEMENT, PROJECT, TASK AREA & WORK UNIT NUMBERS 62201F 1367 02 33
11. CONTROLLING OFFICE NAME AND ADDRESS Air Force Flight Dynamics Laboratory Air Force Systems Command Wright-Patterson AFB, Ohio 45433		12. REPORT DATE November 1975
		13. NUMBER OF PAGES 48
14. MONITORING AGENCY NAME & ADDRESS(If different from Controlling Office)		15. SECURITY CLASS. (of this report) UNCLASSIFIED
136702		15a. DECLASSIFICATION/DOWNGRADING SCHEDULE

16. DISTRIBUTION STATEMENT (of this Report)

Approved for public release; distribution unlimited.

50 p.

17. DISTRIBUTION STATEMENT (of the abstract entered in Block 20, if different from Report)

18. SUPPLEMENTARY NOTES

19. KEY WORDS (Continue on reverse side if necessary and identify by block number)

Aircraft Dynamic Response
Atmospheric Turbulence
Power Spectral Techniques
Vertical Motion and Pitch
Nonsteady Lift Effects

20. ABSTRACT (Continue on reverse side if necessary and identify by block number)

Gust response analysis based upon power spectral techniques is made for an airplane having the two degree of freedom of vertical motion and pitch. A rather unique formulation of the equations of motion is made, wherein the aerodynamic loads are treated as dependent variables, as are the vertical and pitching motions. Nonsteady lift effects, finite span effects, tail downwash effects, and gust lag effects are all taken into account over the complete frequency range of concern.

DD FORM 1473 EDITION OF 1 NOV 65 IS OBSOLETE
1 JAN 73

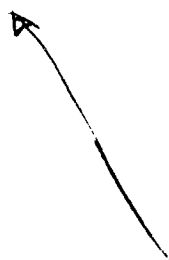SECURITY CLASSIFICATION OF THIS PAGE (When Data Entered)

20. ABSTRACT (cont.)

It is found that the inclusion of pitch considerably alters the response from that found for the case of vertical motion alone. In general, pitch is found to cause a significant attenuation of the response at low frequencies. One of the important findings of the study is the fact that the gust response for the two-degree-of-freedom case can be expressed in a form which is essentially independent of the integral scale of turbulence. Variations in geometric parameters of the airplane, such as tail moment arm, or radius of gyration in pitch, are considered to obtain an idea of the sensitivity of the gust response to these parameters.

PREFACE

This report was prepared by Aeronautical Research Associates of Princeton, Inc., Princeton, New Jersey, under Air Force Contract F33615-75-C-3030. The contract was initiated under Project No. 1367, Task No. 136702, "Structural Design Criteria for Atmospheric Turbulence." The work was administered under the direction of the Air Force Flight Dynamics Laboratory, Air Force Systems Command, Wright-Patterson Air Force Base, Ohio, Mr. Paul L. Hasty (AFFDL/FBE), Project Engineer.

The work reported in this study was conducted by Aeronautical Research Associates of Princeton, Inc. with Dr. John C. Houbolt as principal investigator, and covers the period 1 November 1974 to 30 September 1975. The report was submitted by the author in November 1975.

The contractor's report number is A.R.A.P. 256.

TABLE OF CONTENTS

v

LIST OF SYMBOLS

a	slope of the lift curve
A	structural response parameter, $\sigma_x = A\sigma_w$; also, aspect ratio, $A = \dfrac{b^2}{S}$
b	wing span
c	wing chord
c_t	chord of horizontal tail
e	distance from c.g. to 1/4-chord position of wing
e_t	distance from c.g. to 1/4-chord position of tail
k	reduced frequency, $k = \dfrac{\omega c}{2U}$
K	gust response factor
L	integral scale of turbulence
m	airplane mass
Δn	incremental load factor due to gusts
N_o	number of upward crossings per second of 1-g load level due to gusts
p	aerodynamic loading
P_n	magnitude of line load, $P_n = \lambda p_n$
r	radius of gyration in pitch
s	nondimensional time or distance, $s = \dfrac{2x}{c} = \dfrac{2Ut}{c}$
S	wing area
U	airplane velocity
w	downwash velocity
w_o	magnitude of sinusoidal gust
W	airplane weight
z	vertical displacement of airplane

LIST OF SYMBOLS (concluded)

α line load length, $\alpha = \frac{\lambda}{c}$; also angle of attack

λ length of aerodynamic line load

λ_t length of aerodynamic line load on tail

μ mass parameter

ρ air density

σ_x rms value of variable x

ϕ pitch angle

$\phi_w(k)$ power spectrum of vertical gust velocities

ω angular frequency

LIST OF ILLUSTRATIONS

Figure

I.   INTRODUCTION

In the treatment of the response of aircraft to atmospheric turbulence, a common assumption has been to consider that the aircraft system is represented by a rigid body with the single degree of freedom of vertical motion only. Many design studies and design charts have been based on this assumption; for example, references 1, 2 and 3. The consideration of several degrees of freedom, including vertical motion, pitch, and flexible modes, has generally been limited to isolated treatments of specific aircraft, such as shown in reference 4. It should be noted that the results for the response parameters A and N_0 obtained from a multi-degree-of-freedom analysis may differ considerably from the results of a single degree-of-freedom analysis; the results should therefore not be used interchangeably, as is often done.

The general intent of multimode treatments is to bring out changes in response or amplification effects due to flexibility. Such response analyses thus tacitly concentrate on higher frequency effects. It is found, however, that the low frequency effects may be even more significant than the high frequency effects. Consider figure 1. Flexibility may cause a rather large change in the airplane transfer function at the higher frequencies (as compared with the rigid body result), but this change is weighted by rather small values of the input spectrum. By contrast, the change in the transfer function at low frequencies due to including pitch may appear small, but this change is weighted by very large values of the input spectrum. The resulting effect which shows up in the output spectrum of including or not including pitch may therefore be greater than flexibility effects.

The effect of including pitch may be seen somewhat by physical reasoning. If vertical motion only is considered, the airplane tends to follow or go up and down with the gusts in the low frequency range. With pitch included, however, the airplane acts as a weathercock at low frequencies, with the result that there is virtually no vertical motion response. In effect, the inclusion of the degree-of-freedom of pitch with vertical motion causes the response spectrum to shift to higher frequencies.

The basic point being made is that not enough attention has been focused on the low frequency end of the gust response spectrum. Reference 5 gives a treatment involving vertical motion and pitch. The analysis is based, however, on a stability derivative approach, and it is not known how well the analysis applies at intermediate frequencies, where most of the gust response power seems to appear. The purpose of this proposed investigation is thus to make a systematic study of gust response, based on spectral techniques wherein both the degrees-of-freedom of vertical motion and pitch are included. The aim is to derive parametric-type charts which allow for the easy evaluation of the response parameters A and N_o .

1

II. THEORETICAL DEVELOPMENT

The inclusion of pitch with vertical motion considerably com-
plicates the aerodynamics and the dynamics of the airplane,
especially in contrast to the vertical motion analysis given in
reference 2. The aerodynamic development given herein includes the
following effects:

1. Nonsteady lift effect both due to airplane motion and due
    to gust penetration.

2. Finite span effects.

3. Downwash effects on the tail (with oscillatory effects
    included).

4. The time lag associated with the gusts encountering the
    tail at a later time than the wing.

It may be noted that the developments which follow represent a
rather unique formulation of the equations of motion.

A. Aerodynamic Loading

The aerodynamic forces used herein are found in accordance
with the analysis given in reference 6. The development in this
reference is in terms of the average downwash over a finite span
interval due to a concentrated or point aerodynamic load. An
equivalent procedure is to establish the downwash at a point due
to a uniform line load of finite length. This equivalent procedure
is used herein.

The aerodynamic loading considered in this study is shown in
figure 2; this figure also serves to indicate some of the notation
used. It is to be noted that an aim in this study was to keep the
number of aerodynamic loads to a minimum, yet still of sufficient
generality so as to represent overall loads and moments on the
airplane in a realistic manner (the aim is to establish the air-
plane dynamics reasonably well, not to obtain precise airloads over
the wing). The wing loading is seen to be represented by two line
loads, while a single line load is used for the tail. Later
examples will show that this rather "crude" representation of the
aerodynamics gives fairly accurate loads. The following consider-
ation serves to indicate that two line loads on the wing should be
adequate for taking into account the gust frequency components of
concern. Consider a gust frequency component with wavelength λ ;
spatial frequency then follows as

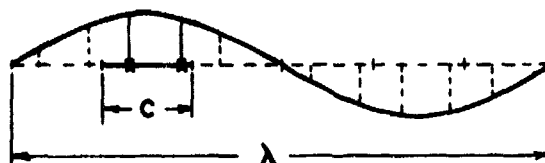$$\Omega = \frac{\omega}{V} = \frac{2\pi}{\lambda}$$

These relations lead in turn to

$$\frac{\lambda}{c} = \frac{\pi}{k}$$

2

where $k = \frac{\omega c}{2U}$. Past gust studies (reference 2) show that the largest value of k of concern is around $k = .5$; this value leads to the shortest wavelength of concern of

$$\frac{\lambda}{c} \approx 6$$

Relative to this shortest wavelength, two control or downwash points in the chordwise direction would appear as in the following sketch.

Effectively, one wavelength of the shortest gust component is represented by 12 points, which is a fairly good approximation. All lower k values, or longer wavelengths, where there is more response power, are of course represented even more accurately.

The control or downwash points, two on the wing, one on the tail, that are used in the subsequent development are also shown in figure 2. Definition of two aspect-ratio-type terms are

$$\alpha = \frac{\lambda}{c}$$
$$\alpha_t = \frac{\lambda_t}{c_t}$$

If the wing is assumed to behave in the fashion of an elliptical wing, some additional parameters of convenient use may be established, such as the following:

$$S = c\lambda = \frac{\pi c b}{4}$$

$$\lambda = \frac{\pi}{4} b$$

$$A = \frac{b^2}{S} = \frac{16}{\pi^2} \frac{\lambda}{c} = \frac{16}{\pi^2} \alpha$$

Use will be made of these relations in later examples.

3

B. Aerodynamic Forces

The aerodynamic forces that are of concern in this study are derived in this section. The strength of the wake potential due to a uniform line load of intensity p , see figure 3(a), is given by

$$\phi_o = - \frac{p}{\rho U} \, e^{- \frac{i \omega x}{U}} \tag{1}$$

Since this line load extends from $y = - \frac{\lambda}{2}$ to $y = \frac{\lambda}{2}$, the total load is given by

$$P = p\lambda \tag{2}$$

For present application purposes, we need the downwash values along the x-axis, both ahead of and behind the line load. To establish these downwash values, use is made of the potential for a unit dipole source, given by

$$\phi_d = - \frac{1}{4\pi} \, \frac{z}{(x^2+y^2+z^2)^{3/2}}$$

The downwash in the z = 0 plane that is associated with this dipole source, for regions outside the origin, is given by

$$w = - \frac{1}{4\pi} \, \frac{1}{(x^2+y^2)^{3/2}} \tag{4}$$

By equations (1) and (3), the downwash ahead of the line load (for y = 0) is given by (see figure 3(b))

$$w = \frac{p}{4\pi\rho U} \int_{-\lambda/2}^{\lambda/2} \int_{0}^{\infty} e^{- \frac{i \omega \xi}{U}} \frac{1}{\left[(x+\xi)^2+y^2\right]^{3/2}} \, d\xi dy \tag{5}$$

This equation may be converted to the following result

$$w = \frac{P}{\pi\rho U c\lambda} \, e^{iks}(C_1 - iS_1) \tag{6a}$$

where

$$C_1 = \int_{s}^{\infty} \frac{\alpha \cos ks}{s^2\sqrt{s^2+\alpha^2}} \, ds \tag{6b}$$

4

$$S_1 = \int_s^\infty \frac{\alpha \sin ks}{s^2\sqrt{s^2 + \alpha^2}} \, ds \tag{6c}$$

in which
$$\alpha = \frac{\lambda}{c}$$

$$k = \frac{\omega c}{2U}$$

$$s = \frac{2x}{c}$$

For the downwash behind (downstream) the line load we first establish the potential in the field due to the strength given by equation (1). By equations (1) and (3) the field potential for $y = 0$ is given by (see figure 3(c))

$$\phi = \frac{p}{4\pi\rho U} \int_{-\lambda/2}^{\lambda/2} \int_0^\infty e^{-\frac{i\omega\xi}{U}} \frac{z}{\left[(x-\xi)^2 + y^2 + z^2\right]^{3/2}} \, d\xi \, dy \tag{7}$$

It is convenient to change the variable of integration in the x direction, and then rewrite the equation so that it assumes the form

$$\phi = \frac{pe^{-\frac{i\omega x}{U}}}{4\rho U} \left[\int_{-\infty}^\infty \int_{-\infty}^\infty f \, dx \, dy - \int_{-\lambda/2}^{\lambda/2} \int_x^\infty f \, dx \, dy - 2\int_{\lambda/2}^\infty \int_{-\infty}^\infty f \, dx \, dy \right] \tag{8}$$

where
$$f = \frac{1}{\pi} e^{\frac{i\omega x}{U}} \frac{z}{(x^2+y^2+z^2)^{3/2}}$$

By transforms 918.5 and 867 in reference 7, the first term within the brackets of equation (8) can be integrated, the result being

simply $2e^{-\frac{\omega}{U} z}$; equation (8) thus appears

5

$$\phi = \frac{\text{pe}^{-\frac{i\omega x}{U}}}{4\rho U}\left[2e^{-\frac{\omega z}{U}} - \int_{-\lambda/2}^{\lambda/2} \int_{x}^{\infty} f\,dxdy - 2\int_{\lambda/2}^{\infty} \int_{-\infty}^{\infty} f\,dxdy\right] \quad (9)$$

The downwash in the $z = 0$ plane indicated by this equation is

$$w = \frac{\partial \phi}{\partial z}\Big)_{z=0} = \frac{\text{pe}^{-\frac{i\omega x}{U}}}{4\rho U}\left[-2\frac{\omega}{U} - \int_{-\lambda/2}^{\lambda/2} \int_{x}^{\infty} f_1\,dxdy - 2\int_{\lambda/2}^{\infty} \int_{-\infty}^{\infty} f_1\,dxdy\right] \quad (10)$$

where

$$f_1 = \frac{1}{\pi} e^{\frac{i\omega x}{U}} \frac{1}{(x^2 + y^2)^{3/2}}$$

Equation (10) may be integrated further, and then reduced to the following result

$$w = -\frac{\text{Pe}^{-iks}}{\pi\rho U c\lambda} (C_o + C_1 + iS_1) \quad (11a)$$

where

$$C_o = \pi k + 2\int_0^{\infty} \frac{\cos ks}{s^2}\left(1 - \frac{\alpha}{\sqrt{s^2+o^2}}\right) ds \quad (11b)$$

and where k and s are as before.

Equations (6) and (11) are the basic equations used herein for the evaluation of the downwash that results from the aerodynamic loads on the wing and the tail. For later application, it is convenient to introduce a simplified but descriptive notation of these equations, both in application to the wing and the tail. For the wing, let

$$w_m = \frac{P_n}{\pi\rho U c\lambda}(\alpha_{mn} + i\beta_{mn}) \quad (12)$$

where the notation is interpreted as the downwash at point m due to a load at point n. The definitions for α_{mn} and β_{mn} are as follows: For a downwash point ahead of the line load we have,

6

from equation (6)

$$\alpha_{mn} + i\beta_{mn} = e^{iks}(C_1 - iS_1) \tag{13}$$

while for a downwash point behind the line load, equation (11) gives the definition

$$\alpha_{mn} + i\beta_{mn} = -e^{iks}(C_0 + C_1 + iS_1) \tag{14}$$

It is to be noted that the values of s used in equation (13) is based on the absolute value of the distance the downwash point is ahead of the line load; likewise s in equation (14) is based on the absolute value of the distance the downwash point is behind the line load.

In the application of equations (6) and (11) to the tail, consideration must be given to the fact that λ and c may be different. For the tail

$$s_t = \frac{2x}{c_t}$$

$$k_t = \frac{\omega c_t}{2V}$$

and to express the k values in terms of a common value, we write

$$k_t = \frac{c_t}{c} k \tag{15}$$

In this study downwash points on the tail ahead of the line load are not considered. For downwash points behind the tail line load, equations (11) and (15) give

$$w_{mn} = \frac{P_n}{\pi\rho U c_t \lambda_t} (\alpha_{mn} + i\beta_{mn}) \tag{16a}$$

where

$$\alpha_{mn} + i\beta_{mn} = -e^{i\frac{c_t}{c} k s_t}(C_{0_t} + C_t + iS_t) \tag{16b}$$

$$C_t = \int_{s_t}^{\infty} \frac{\alpha_t \cos \frac{c_t}{c} ks}{s^2\sqrt{s^2 + \alpha_t^2}} ds \tag{16c}$$

7

$$S_t = \int_{s_t}^{\infty} \frac{\alpha_t \, \sin \frac{c_t}{c} ks}{s^2 \sqrt{s^2 + \alpha_t^2}} \, ds \qquad (16d)$$

$$C_{s_t} = \pi \frac{c_t}{c} k + 2 \int_0^{\infty} \frac{\cos \frac{c_t}{c} ks}{s^2} \left(1 - \frac{\alpha_t}{\sqrt{s^2 + \alpha_t^2}}\right) ds \qquad (16e)$$

Steady State Check.- As a check on the accuracy that might be expected from the assumed line load distribution used herein, application was made to a wing in a steady state constant angle of attack condition. Two cases were studied: one with a single line load; one with two line loads, as shown in the following central cross sections of the wing.
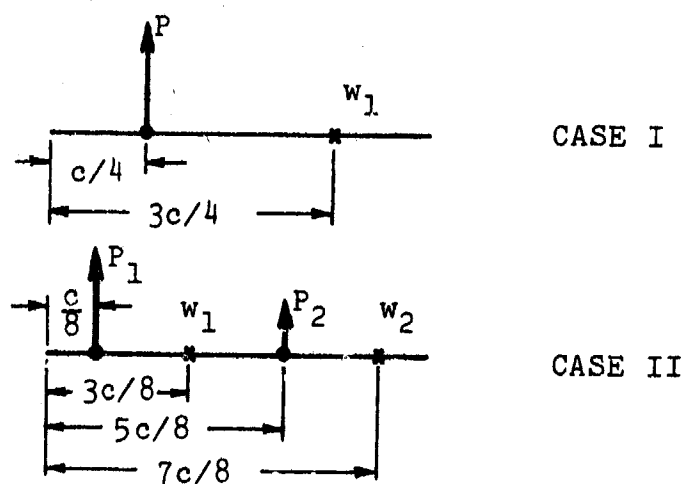
Results obtained by applying equations (6) and (11) are as follows. For Case I, P was found to be given by

$$P = \frac{\alpha}{1 + \sqrt{1 + \alpha^2}} \pi \rho U^2 S \alpha_o$$

where α_o denotes angle of attack.

Consider a wing with aspect ratio $A = 8$, then

$$\alpha = \frac{\pi^2}{16} \times 8 = 4.9348$$

P in turn evaluates to

$$P = .8177\pi\rho U^2 S\alpha_o$$

For an elliptical wing of $A = 8$, and with the use of the factor $\frac{A}{A+2}$ for aspect ratio correction to the slope of the lift curve, P would evaluate to

$$P = .8\pi\rho U^2 S\alpha_o$$

The result obtained from using only a single finite length line load is seen to be only about 2% different than the corresponding exact solution for an elliptic wing.

For Case II, the following results were found:

$$P_1 = .6164\pi\rho U^2 S\alpha_o$$

$$P_2 = .2013\pi\rho U^2 S\alpha_o$$

$$\sum P_n = P = .8177\pi\rho U^2 S\alpha_o$$

The result is seen to be the same as for Case I.

C. Equations of Motion

In reference to figure 2, the equations for vertical and pitching motion of the airplane are

$$m\ddot{z} = P_1 + P_2 + P_3 \tag{17}$$

$$mr^2\ddot{\phi} = (e + \frac{c}{8})P_1 - (\frac{3c}{8} - e)P_2 - e_t P_3 \tag{18}$$

The vertical displacements of the control points w_1, w_2, and w_3 are given by

$$z_1 = z + (e - \frac{c}{8})\phi \tag{19}$$

$$z_2 = z + (e - \frac{5c}{8})\phi \tag{20}$$

$$z_3 = z - (e_t + \frac{c_t}{2})\phi \tag{21}$$

9

The downwash at the control points is due to three sources: the vertical velocity movement as can be found from equations (19), (20), and (21), the instantaneous angle of attack, and the sinusoidal gust which is assumed to flow over the airplane (for purposes of determining the frequency response function due to sinusoidal gust encounter). Consideration of these three sources yields the downwash values

$$w_1 = \dot{z} + (e - \frac{c}{8})\dot{\phi} - U\phi - w_o \tag{22}$$

$$w_2 = \dot{z} + (e - \frac{5c}{8})\dot{\phi} - U\phi - w_o e^{-i\frac{\omega c}{2U}} \tag{23}$$

$$w_3 = \dot{z} - (e_t + \frac{c_t}{2})\dot{\phi} - U\phi - w_o e^{-i\frac{\omega}{U} e_1} \tag{24}$$

where w_o is the magnitude of the sinusoidal gust, and

$$e_1 = e_t + e - \frac{c}{8} + \frac{c_t}{2}$$

We note that these equations take into account the lag in the time that the sinusoidal gust is felt at points 2 and 3 relative to point 1.

By equations (12), (13), (14) and (16) the downwash at the control points, when expressed in terms of the loads P_1, P_2, and P_3, may also be written as

$$w_1 = \frac{1}{\gamma}\left[(\alpha_{11} + i\beta_{11})P_1 + (\alpha_{12} + i\beta_{12})P_2\right] \tag{25}$$

$$w_2 = \frac{1}{\gamma}\left[(\alpha_{21} + i\beta_{21})P_1 + (\alpha_{11} + i\beta_{11})P_2\right] \tag{26}$$

$$w_3 = \frac{1}{\gamma}\left[(\alpha_{31} + i\beta_{31})P_1 + (\alpha_{32} + i\beta_{32})P_2 + \frac{S}{S_t}(\alpha_{33} + i\beta_{33})P_3\right]$$

$$\tag{27}$$

where $\gamma = \pi\rho US$; note $\alpha_{22} = \alpha_{11}$, and $\beta_{22} = \beta_{11}$. We note that the downwash on the tail due to the wing loads is taken into account; the downwash on the wing due to the tail load is ignored, however, on the basis that this effect should be small.

We now set equations (22), (23), and (24) equal to equations (25), (26), and (27). The three equations thus formed, together with equations (17) and (18) then form a set of 5 equations with 5 unknowns, z, ϕ, P_1, P_2 and P_3. The equations so found are given in Table I (in a nondimensional representation, and with w_o

10

set equal to unity to apply to a unit sinusoidal gust). The
application of equations (12), (13), (14) and (16) to the three
specific control points shown in figure 2 involved the choice of
s values as follows:

For	s
α_{11} & β_{11}	$\frac{1}{2}$
α_{12} & β_{12}	$\frac{1}{2}$
α_{21} & β_{21}	$\frac{3}{2}$
α_{31} & β_{31}	$\frac{1}{4} + 2(\frac{e}{c} + \frac{e_t}{c}) + \frac{c_t}{c}$
α_{32} & β_{32}	$-\frac{3}{4} + 2(\frac{e}{c} + \frac{e_t}{c}) + \frac{c_t}{c}$
α_{33} & β_{33}	$s_t = 1$

It should be noted that the equations given in Table I repre-
sent a rather unique formulation of the gust response problem. We
do not establish the loads that are due to airplane motion and due
to gust encounter, and then feed these loads into the dynamical
equations of motion to establish t   frequency response, as is
usually the conventional approach. Here, we let the loads be un-
known quantities just as the variables z and ϕ . All aero-
dynamic effects - nonsteady lift effects, spanwise induction
effects, tail downwash, and the lag of the gusts in traveling from
the wing to the tail - are all automatically taken into account.
For solution, all we need to solve for is ωz , from which the

vertical load factor follows as $\frac{\omega^2 z}{g}$. Direct determination of
the loads P_1 , P_2 , and P_3 is completely bypassed. We note,
however, that the equations allow for the ready determination of
the aerodynamic loads on the airplane, if desired. All we have to
do is consider the last 3 equations; solution of these equations
for P_1 , P_2 , and P_3 gives the loads that are due to vertical
motion ωz , or due to pitch ϕ , or due to gust encounter w_o .

We might note how the extension to two degrees of freedom has
greatly increased the number of airplane parameters involved. For
the case of the single degree of freedom of vertical motion, the

airplane can be described by one parameter only, the mass parameter μ (reference 2). For the case of the two degrees of freedom of vertical motion and pitch, at least seven parameters are required to describe the airplane, namely:

$$\mu \ , \ \frac{r}{c} \ , \ \frac{e}{c} \ , \ \frac{e_t}{c} \ , \ \frac{\lambda}{c} \ , \ \frac{\lambda_t}{c_t} \ , \text{ and } \ \frac{c_t}{c} \ .$$

where r is the radius of gyration for pitching inertia. This large number of parameters essentially precludes the generation of generalized parametric charts.

D. Evaluation of the Response Spectrum

The evaluation of the response spectrum follows readily from the equations in Table I as follows. First, consider the determination of the frequency response function for c.g. vertical acceleration due to sinusoidal gust encounter. Through use of the equations given in Table I, the resulting c.g. acceleration is given as

$$\Delta n = \frac{\omega^2 z}{g}$$

The output spectrum for Δn is then

$$\phi_{\Delta n} = |\Delta n|^2 \phi_w = |\frac{\omega^2 z}{g}|^2 \phi_w \tag{28}$$

where ϕ_w is the gust input spectrum. The rms value for Δn follows as

$$\sigma_{\Delta n} = \left[\int_0^{k_c} |\frac{\omega^2 z}{g}|^2 \phi_w dk \right]^{1/2} \tag{29}$$

where k_c is some cut-off frequency (to be discussed subsequently). We wish to rearrange equation (29) so that it has a form similar to that used in past gust studies; specifically, the following form is sought

$$\sigma_{\Delta n} = \frac{\pi \rho S U}{W} K \sigma_1$$

$$= \frac{U}{cg} \frac{K}{\mu} \sigma_1 \tag{30}$$

where

$$\mu = \frac{W}{\pi \rho c g S}$$

and where K is in the nature of an alleviation factor, and σ_1 is some rms gust input value. When the rearrangement is made,

we find that

$$K = \left[\int_0^{k_c} f_1 \frac{\phi_w}{\sigma_1^2} \, dk \right]^{1/2} \tag{31}$$

where

$$f_1 = 4\mu^2 k^2 |\omega z|^2$$

The value of k_o which is associated with the number of upward crossings per second according to the equation

$$N_o = \frac{U}{\pi c} k_o$$

follows as

$$k_o = \left[\frac{\int_0^{k_c} k^2 f_1 \frac{\phi_w}{\sigma_1^2} \, dk}{\int_0^{k_c} f_1 \frac{\phi_w}{\sigma_1^2} \, dk} \right]^{1/2} \tag{32}$$

For use in computational studies, the value of k_c used will be the rule-of-thumb value that is discussed in reference 8, namely

$$k_c = \frac{\pi}{A}$$

where A as used in this definition refers to wing aspect ratio.

The gust input spectrum that is adopted herein is given by the equation

$$\phi_w(k) = \frac{\sigma_w^2 2L}{\pi c} \frac{1 + \frac{8}{3}\left(1.339 \frac{2L}{c} k\right)^2}{\left[1 + \left(1.339 \frac{2L}{c} k\right)^2\right]^{11/6}}$$

This equation may be rearranged so as to yield the result

$$\frac{\phi_w(k)}{\sigma_1^2} = \frac{\left(\frac{2L}{c}\right)^{5/3}\left[1 + \frac{8}{3}\left(1.339 \frac{2L}{c} k\right)^2\right]}{\left[1 + \left(1.339 \frac{2L}{c} k\right)^2\right]^{11/6}} \tag{33}$$

13

where

$$\sigma_1^2 = \frac{\sigma_w^2}{\pi \left(\frac{2L}{c}\right)^{2/3}} \tag{34}$$

A plot of equation (33) is shown in figure 4. We note that the rearrangement was made so that all the spectra pass through the same values at high k, regardless of the value of $2L/c$. This alteration in spectrum definition is made because of the belief that results obtained may be fairly insensitive to or independent of the $2L/c$ value used.

14

III. RESULTS

A. Check with One-Degree-of-Freedom Case

As a partial check of the equations given in Table I, solution was made for the case where the pitching motion was set equal to zero (set $\phi = 0$ and strike out the second equation); thus, a solution for vertical motion response alone is obtained. Typical results for the f_1 function are shown in figure 5. The open points are the results for $\mu = 20$ and $\mu = 100$ as given by the single-degree-of-freedom treatment of reference 2. It is noted that good agreement is obtained throughout. The slight difference in results is probably due to the fact that the analysis presented herein takes into account lag in lift and gust penetration effects in different but perhaps better fashion. The main point of the figure is that it serves to indicate that the basic equations are correct.

B. Results for Basic Cases Studied

To establish an understanding of how pitch influences the airplane response due to gusts, four cases covering a range in the basic parameters were studied. The following table indicates the parameters used in these four basic cases.

Case	A	α	α_t	$\dfrac{e}{c}$	$\dfrac{e_t}{c}$	$\dfrac{c_t}{c}$	$\dfrac{\lambda_t}{\lambda}$	$\dfrac{S}{S_t}$	$\dfrac{r}{c}$
I	6	3.701	2.056	0	3.3	.6	1/3	5	1
II	6	3.701	2.056	.15	3.15	.6	1/3	5	1
III	10	6.169	3.427	0	3.3	.6	1/3	5	1
IV	10	6.169	3.427	.15	3.15	.6	1/3	5	1

These cases were chosen mainly to bring out the effect of aspect ratio A, and of the importance of the c.g. position as given by $\dfrac{e}{c}$.

One of the most significant results of the present study is shown in figure 6. In this figure the f_1 function, which represents the square of the amplitude of the frequency response function, is given for the airplane with two degrees of freedom (vertical motion and pitch) and for the airplane with vertical motion only. Two significant points are seen. First, there is a

15

very pronounced peak for the two-degree-of-freedom airplane, associated with the short period mode. Second, the frequency response function for the vertical motion only case is very large at low frequencies, whereas the function is negligible at low frequencies for the two-degree-of-freedom case, due to the weathercocking of the airplane, as mentioned in the introduction. Gust power at the low frequencies is thus significantly lower for the two-degree-of-freedom airplane as compared with the airplane with the single degree of vertical motion only.

Figure 7 compares how the response power for c.g. vertical acceleration is distributed with frequency for the vertical motion only case and for the airplane with pitch and vertical motion. In this figure $kf_1\phi_w$ is plotted against log k ; this type plot is significant because it shows how the response power, as given by the area under the curves as seen, is distributed with frequency. Two points of significance are noted. First, the major response power for the two-degree-of-freedom case appears at much higher frequencies in comparison to the vertical motion only case. Second, the response for the vertical motion only case is strongly dependent on the $\frac{2L}{c}$ ratio; for the two-degree-of-freedom case, the response appears to be rather insensitive to the value of $\frac{2L}{c}$.

Values of K and k_o obtained for Case III are shown as a function of the mass parameter μ in figures 8 and 9. In the study of these figures we should keep in mind that practical values of $\frac{2L}{c}$ appear to be 100 or greater (suppose L = 1000 ft, and c = 10 ft; then $\frac{2L}{c}$ = 200). Thus, if we discount the $\frac{2L}{c}$ = 50 curve, and consider μ value less than about 100, which represents the range of practical interest, we see that the results for K and k_o can be represented essentially by single curves independent of $\frac{2L}{c}$. This observation is in marked contrast to results that are found for the vertical motion case (reference 2). The fact that the consideration of both pitch and vertical motion seems to give gust response results which are essentially independent of the turbulent scale L is a significant finding of this study. The results suggest that we can eliminate L , which has been the subject of much controversy over the past several years, as one of the parameters to be considered in the design for gusts.

Results found for Cases I, II and IV are very similar trendwise to the results shown in figures 8 and 9, and are thus not presented. Examination of the results for all four cases indicates that the K or k_o curve for $\frac{2L}{c}$ = 200 can be taken for practical purposes as the single curve which represents the results for all values of $\frac{2L}{c}$ greater than 100 . On this basis, figures 10 and 11

16

give the $\frac{2L}{c} = 200$ results for K and k_o for all the basic cases studied. These figures indicate that gust response is dependent to some extent on wing aspect ratio and on c.g. position, as might be expected.

C. Results for Parameter Variations

The basic cases studied in the previous section covered mainly aspect ratio and c.g. position effects. In this section results are given for a systematic variation of other airplane configuration parameters. The main intent is to gain an idea of the sensitivity of gust response to the various parameters (we see that the mass parameter μ is still a very significant parameter). Six cases, as listed in the following table, were studied.

Case	$\frac{e_t}{c}$	$\frac{r}{c}$	$\frac{S}{S_t}$
Nominal	3.3	1	5
A	3.63	1	5
B	2.97	1	5
C	3.3	1	4.5
D	3.3	1	5.5
E	3.3	.9	5
F	3.3	1.1	5

Common parameters to all six cases were $A = 10$, $\frac{e}{c} = 10$. Cases A and B represent a 10 percent increase and a 10 percent decrease in the tail moment arm relative to the nominal case. In cases C and D the ratio of wing area to tail area is decreased and increased 10 percent. Cases E and F represent a 10 percent decrease and a 10 percent increase in the radius of gyration in pitch.

Results for K and k_o are shown for the six cases in figures 12 and 13, as obtained using $\frac{2L}{c} = 200$. There is some variation in the results, but, in general, the variation is small. In the range of μ of practical interest, say up to μ of about 60 , it would appear feasible to represent the results by a single curve, with errors less than 5 percent.

17

D. Effects of Downwash on the Tail

To study how important tail downwash effects are, two cases were studied, one with tail downwash effects included, one with the effects removed. In reference to the equations given in Table I, the α_{31} , β_{31} , α_{32} , and β_{32} terms are associated with tail downwash effects. To neglect the influence of downwash on the tail, we simply set these terms equal to zero. Results for $kf_1\phi_w$ as obtained for basic Case III are shown in figure 14. It is seen that the inclusion of downwash causes the peak to shift to a lower frequency, and, as judged by the width of the peak, causes an increase in damping in pitch. Results for K are shown in figure 15. The neglect of downwash is seen to increase the gust response.

E. Comparison with Vertical Motion Only Case

It is of interest to see how the results of the present study compare with previously established results for an airplane having the single degree of freedom of vertical motion only. If we examine equation (33), it can be shown that the K values given in this report are related to the K_ϕ values given in reference 2 by the relation

$$K_\phi = \frac{1}{\sqrt{\pi}\left(\frac{2L}{c}\right)^{1/3}} K \qquad (35)$$

$$= \eta K$$

This realtion yields

$\frac{2L}{c}$	η
50	.1531
100	.1216
200	.0965
400	.0766

By these conversion numbers, values of K_ϕ were established for Case III from figure 8. Results are shown in figure 16 in comparison to the results for the vertical motion only case as taken from reference 2. It is noted that for $\frac{2L}{c} = 50$, the K_ϕ values for the vertical motion case are greater than the K_ϕ values for the two-degree-of-freedom airplane at low μ , but become significantly less at high μ values. For $\frac{2L}{c} = 400$, the K_ϕ values for the vertical motion case are significantly greater over the entire

18

μ range shown. This figure shows that the A values computed for the two-degree-of-freedom case can be considerably different than the A values for the case of vertical motion alone. The implication is that, either in the design for gust or in the reduction of gust data, consistent procedures for establishing A and N_o should be used. For example, it is improper to compare deduced gust data obtained by one investigator using one procedure to compute A with gust data obtained by another investigator who used a different procedure for establishing A .

In figure 17 results for k_o are compared. The solid curve applies to the two-degree-of-freedom case and represents an "average" of the results given in figure 11; the dashed curve applying to the vertical motion only case is taken from reference 8 (A = 8). It is seen, in contrast to the findings for A , that the results for k_o for the two different cases are in fairly good agreement. This is not surprising, since the response spectrum for the two cases is essentially the same at high frequencies (see figure 7), and since k_o depends on a k^2 weighting of the response spectrum.

Because the spectral function used herein was chosen so as to be independent of $\frac{2L}{c}$ for large values of k (see equation (33) and figure 4), the values of K found in this study are different by an order of magnitude than the corresponding K values found in other studies. It is of interest to see what level of gust design velocities should be used with the K of the present report to yield acceleration levels which are similar to those found by the discrete-gust design approach. For the discrete-gust design approach we have

$$\Delta n = \frac{a \rho S V}{2W} K_g U_d$$

Analogous to this equation, and on the basis of the form suggested by equation (30), we write

$$\Delta n = \frac{\pi \rho S V}{W} K U_1$$

where K refers to the values found in this report, and U_1 is the associated design gust velocity. We note that in this report the mass parameter μ is defined in terms of the theoretical lift curve slope of 2π ; in this section we designate this parameter with a subscript, or

$$\mu_1 = \frac{W}{\pi \rho c g S}$$

to distinguish it from the mass parameter used in the discrete-gust approach, namely

19

$$\mu = \frac{2W}{a\rho c g S}$$

As an example, consider an airplane with $a = 5$ and $\mu = 30$. The value μ_1 would then be $\mu_1 = \frac{a}{2\pi} \mu = 23.9$. For $\mu = 30$ the value of K_g is .75 (reference 2), while figure 10 yields a value of K^g of around 4.5 (using $\mu = 23.9$). If we equate the two in equations, and use $U_d = 50$, we find

$$5 \times .75 \times 50 = 2\pi \times 4.5 \times U_1$$

which yields $U_1 = 6.63$. Thus, appropriate gust design values for use with K values as derived in this report are in the neighborhood of 6.5 to 7.0 fps.

It is of interest also to show how the results of the present report are converted so as to yield the structural response parameter A_r as used in reference 3. In reference 3, $\sigma_{\Delta n}$ is given by

$$\sigma_{\Delta n} = A_r \sigma_w$$

If this equation and equation (30) are combined, the following result for A_r is found

$$A_r = \frac{U}{cg} \frac{K}{\mu_1} \frac{\sigma_1}{\sigma_w}$$

where μ_1 is defined as used in this section. Equation (34) yields

$$\frac{\sigma_1}{\sigma_w} = \eta$$

where η is defined as used in equation (35). Thus, A_r becomes

$$A_r = \frac{U}{cg} \frac{K}{\mu_1} \eta$$

For computational purposes, we select a specific value of η; the value suggested is $\eta = .12$ (which corresponds to a $\frac{2L}{c}$ value near 100); the specific A_r equation is thus

$$A_r = .12 \frac{U}{cg} \frac{K}{\mu_1} \tag{36}$$

20

By contrast, the value of A_r as given in references 2 and 3 (single degree of freedom of vertical motion) is given by

$$A_r = \frac{U}{cg} \frac{K_\phi}{\mu} \tag{37}$$

An example application is the following. Suppose that

$$\mu_1 = 23.9 \text{ , or } \mu = 30$$

$$c = 20 \text{ ft}$$

$$U = 500 \text{ fps}$$

The results of this report show that K is approximately 4.5 for $\mu_1 = 23.9$; references 2 or 3 indicate $\frac{K_\phi}{\mu} = .0205$ for $\mu = 30$ (with $\frac{2L}{c} = 100$). Equation (36) then yields

$$A_r = .0175$$

while equation (37) yields

$$A_r = .0159$$

In this specific example, the inclusion of pitch with vertical motion is seen to increase the response parameter A_r as compared to the result for vertical motion alone.

21

IV. CONCLUDING REMARKS

The inclusion of the pitching degree of freedom with vertical motion is found to considerably alter the gust response of an airplane from that obtained by considering the single degree of freedom of vertical motion only. Results can be expressed in a form which is essentially independent of the integral scale of turbulence. It appears feasible, therefore, to eliminate the turbulence scale - which has been the subject of much controversy - as one of the parameters in the design for gust encounter.

At the beginning of this investigation it was the hope that parametric charts could be derived to cover a variety of aircraft configurations. For the case of the single degree of freedom of vertical motion only, results are found to be expressible in terms of a single airplane parameter, the mass ratio μ. Addition of the degree of freedom of pitch is found to increase the number of parameters to at least 7. This large number essentially precludes the generation of parametric charts. On the other hand, the response analysis procedure developed herein leads to fairly simple response equations, as given in Table I. Application of these equations is rather simple with modern computing machines and, thus, results for various configurations can be established almost as quickly as using parametric charts.

To keep results tractable, and to find out the primary significance of including pitch, the analysis was restricted to straight wings, and for incompressible flow. The analysis is easily extended to the compressible flow case. The only change would be the use of different definitions of C_1, S_1, and C_o. The equivalents of these quantities for compressible flow are given in reference 2. The extension to swept wings, or to delta wing planforms, is also quite straightforward, and involves mainly the consideration of the more complex geometry.

The analysis herein was confined to two line loads on the wing and one on the tail. For a more detailed consideration of a specific airplane configuration, the airloads may be expressed in terms of a more detailed grid mesh than used herein. For example, to account for spanwise loading effects in a more precise way than used in this study, three line loads on each half span at each of two chord positions might be used (for symmetric loading, this choice amounts to 6 loads as compared to 2 for the present analysis). The equations that would result would be just as simple as those shown in Table I, and simply would be more in number (one for each wing load assumed, one for each tail load, and two for the z and ϕ motions). It is to be noted that the type of analysis used herein, which leads to the rather simple equations of Table I, can also be used to include flexibility effects; essentially, one more equation would be added for each flexible mode that is considered.

22

TABLE I. EQUATIONS OF MOTION

$$
\begin{bmatrix}
2\mu k & 0 & 1 & 1 & 1 \\[4pt]
0 & 2\mu\,\dfrac{r^2}{c^2}\,x & \dfrac{e}{c}+\dfrac{1}{8} & \dfrac{e}{c}-\dfrac{3}{8} & -\dfrac{e_t}{c} \\[8pt]
-i & -i\!\left(\dfrac{e}{c}-\dfrac{1}{8}\right)+\dfrac{1}{2k} & \alpha_{11}+i\beta_{11} & \alpha_{12}+i\beta_{12} & 0 \\[8pt]
-i & -i\!\left(\dfrac{e}{c}-\dfrac{5}{8}\right)+\dfrac{1}{2k} & \alpha_{21}+i\beta_{21} & \alpha_{11}+i\beta_{11} & 0 \\[8pt]
-i & i\!\left(\dfrac{e_t}{c}-\dfrac{c_t}{2c}\right)+\dfrac{1}{2k} & \alpha_{31}+i\beta_{31} & \alpha_{32}+i\beta_{32} & \dfrac{S}{S_t}\!\left(\alpha_{33}+i\beta_{33}\right)
\end{bmatrix}
\begin{bmatrix}
\omega z \\[6pt]
\omega c\phi \\[6pt]
\dfrac{1}{\gamma}P_1 \\[6pt]
\dfrac{1}{\gamma}P_2 \\[6pt]
\dfrac{1}{i}P_3
\end{bmatrix}
=
\begin{bmatrix}
0 \\[6pt]
0 \\[6pt]
1 \\[6pt]
e^{-ik} \\[6pt]
e^{-iks_1}
\end{bmatrix}
$$

$$\mu = \frac{W}{\pi \rho c g S}$$

$$\gamma = \pi \rho S U$$

$$s_1 = \frac{2e_t}{c} + \frac{2e}{c} - \frac{1}{4} + \frac{c_t}{c}$$

$$k = \frac{\omega c}{2U}$$

23

V.   REFERENCES

1.   Houbolt, John C.:   "Gust Design Procedures Based on Power
     Spectral Techniques," AFFDL-TR-67-74, May 1967.

2.   Houbolt, John C.:   "Design Manual for Vertical Gusts Based on
     Power Spectral Techniques," AFFDL-TR-70-106, July 1970.

3.   Houbolt, John C.:   "Updated Gust Design Values for Use with
     AFFDL-70-106," AFFDL-TR-73-148, November 1973.

4.   Houbolt, John C.:   "Dynamic Response of Airplanes to Atmospheric
     Turbulence Including Flight Data on Input and Response,"
     NASA TR R-199, June 1964.

5.   Peele, Ellwood L.:   "A Method for Estimating Some Longitudinal
     and Lateral Rigid-Body Responses of Airplanes to Continuous
     Atmospheric Turbulence," NASA TN D-6273, August 1971.

6.   Houbolt, John C.:   "Some New Concepts in Oscillatory Lifting
     Surface Theory," AFFDL-TR-69-2, June 1969.

7.   Campbell, George A. and Foster, Ronald M.:   Fourier Integrals
     for Practical Applications.   New York: D. Van Nostrand Co., Inc.,
     July 1954.

8.   Houbolt, John C.:   "Effect of Nonuniform Spanwise Gusts on
     Aircraft Vertical Response," AFOSR TR-74-0754, January 1974.

ϕ_w Input spectrum

$|H|^2$ Airplane transfer function

Vertical motion & pitch

Bending mode

Vertical motion

ϕ_w Response spectrum

Freq., ω
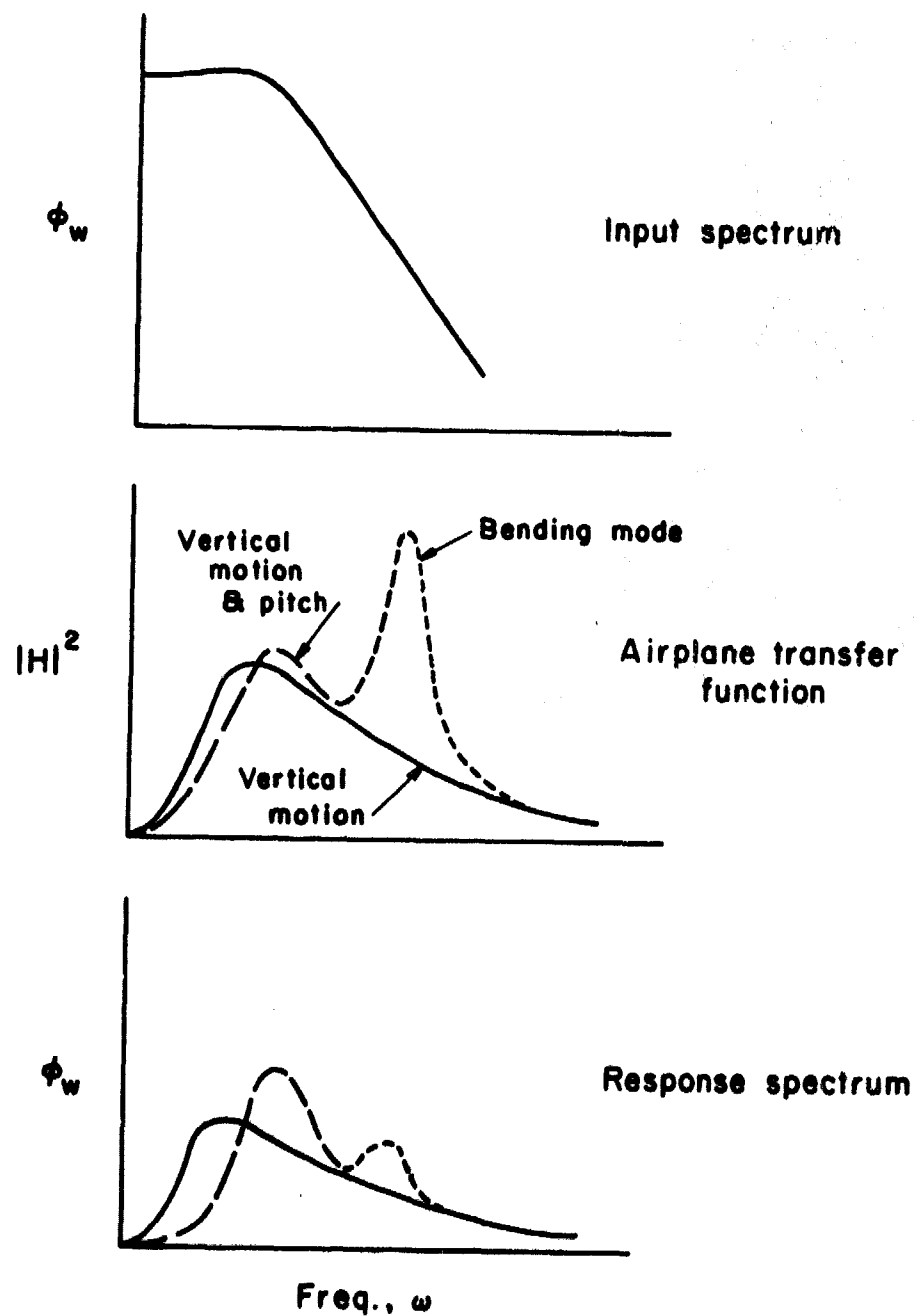
Figure 1.- Influence of Various Degrees of Freedom on Response Spectrum

25
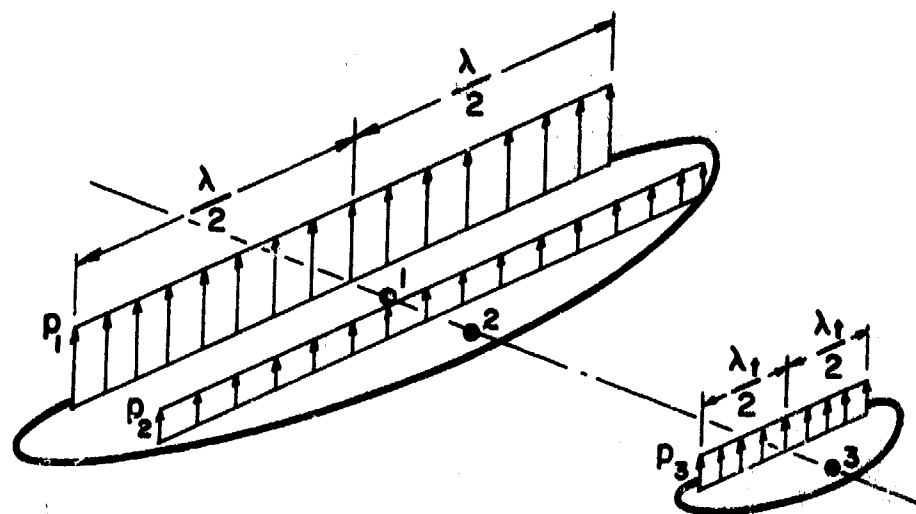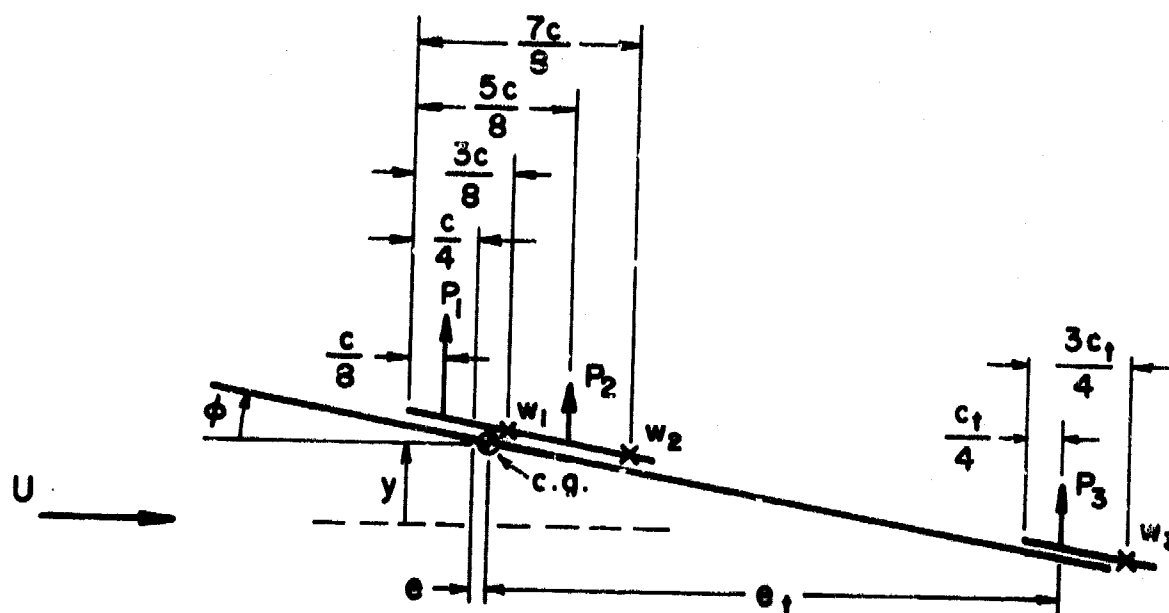
(a) Loading

(b) Geometry

Figure 2.- Loading Distribution and Notation

26

$$\phi_0 = \frac{p}{\rho U} e^{-i\frac{\omega x}{U}}$$
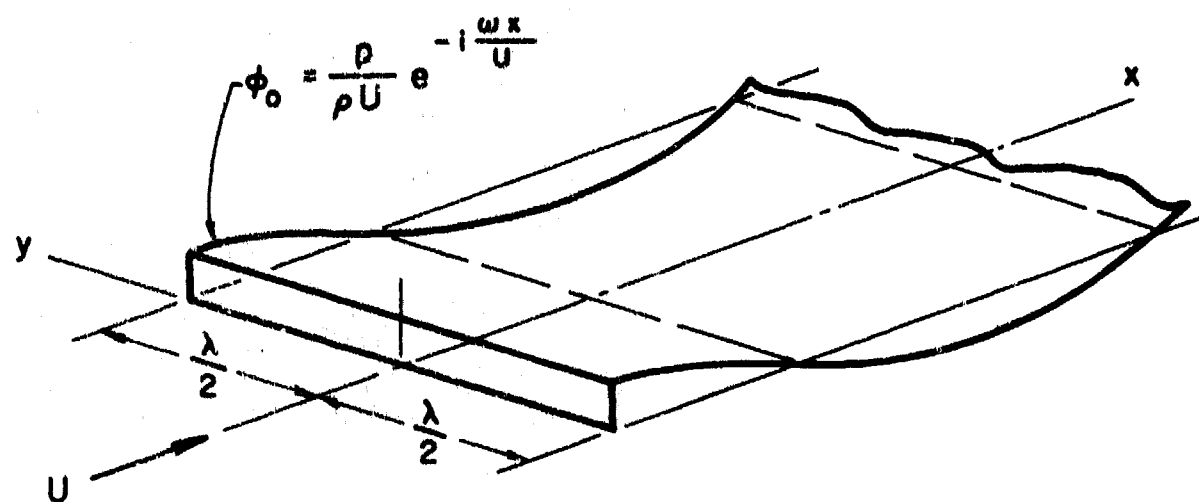
(a) Strength of wake potential for
uniform line loading
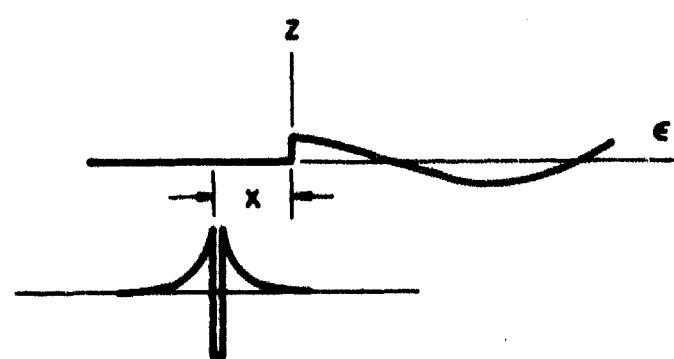
(b) Convolution for downwash
ahead of line load
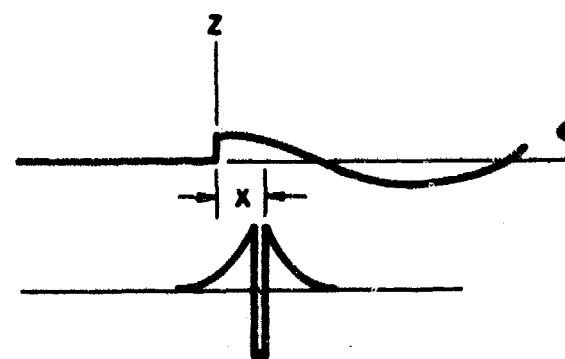
(c) Convolution for downwash
aft of line load

Figure 3.- Geometry for Determination of Downwash Due to Line Load
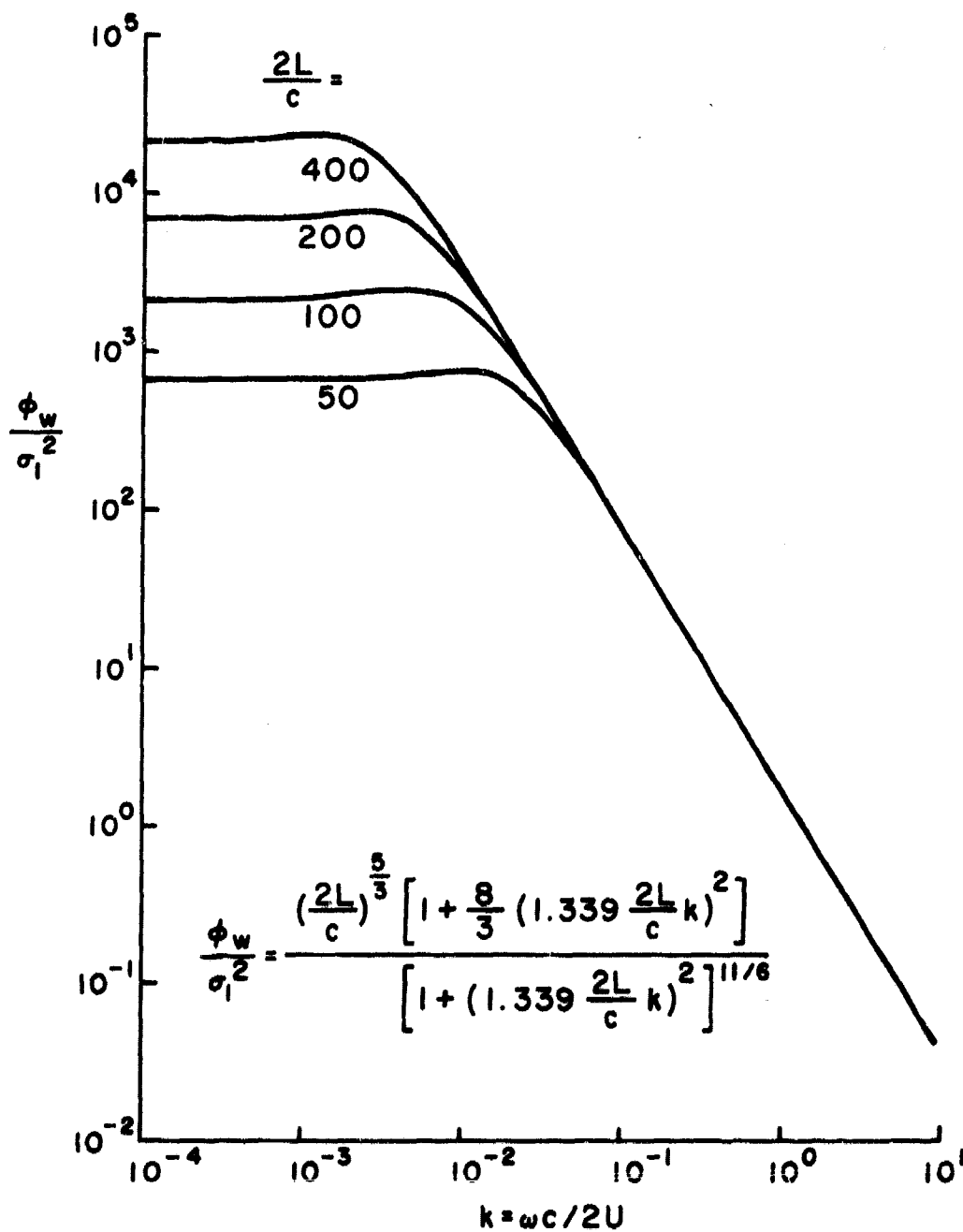
Figure 4.- Gust Input Spectrum Independent of $\frac{2L}{c}$ at High Frequencies

28
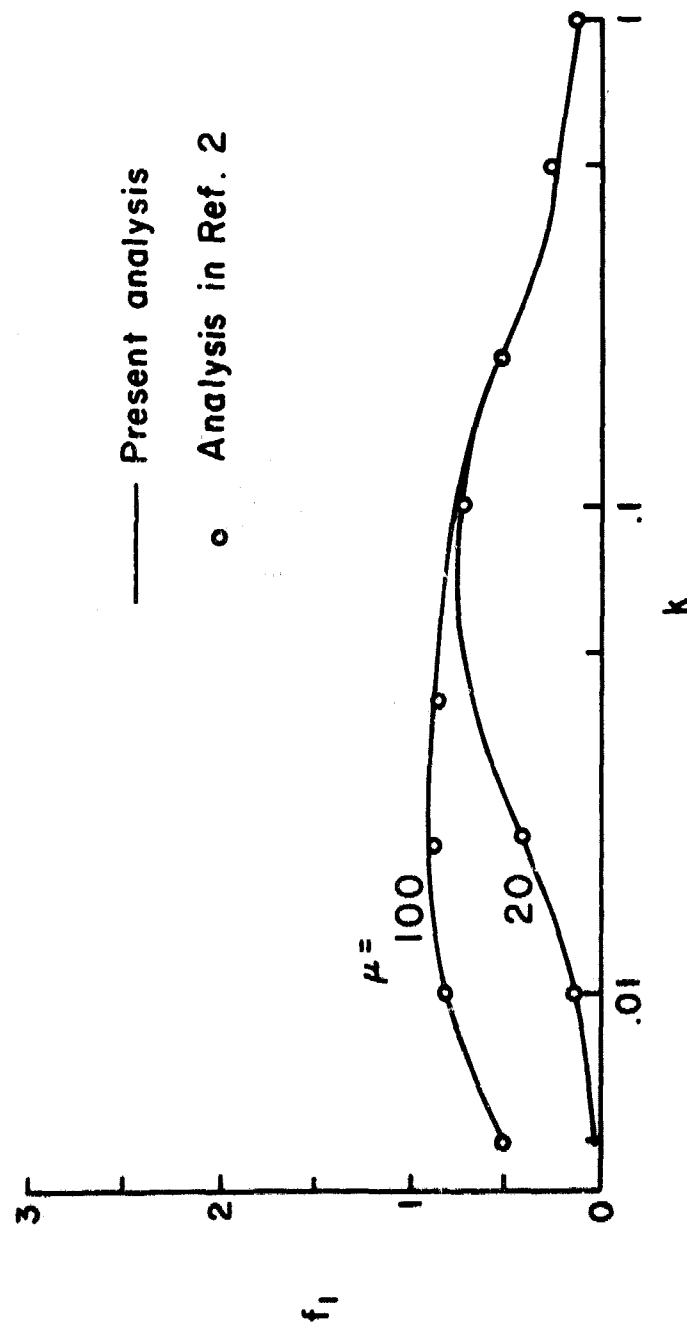
Figure 5.- Airplane Transfer Function Check for One Degree of Freedom
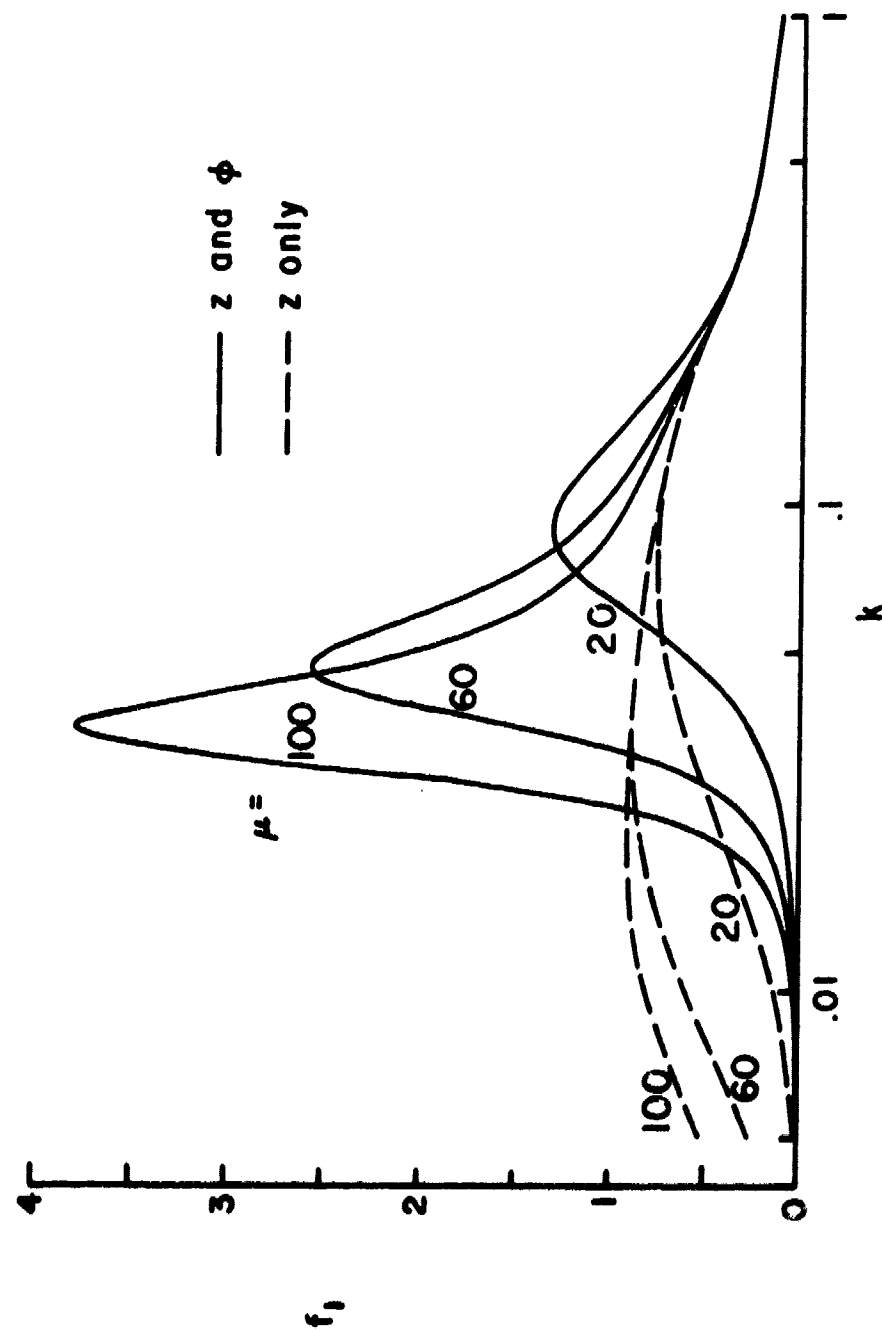
Figure 6.- Comparison of Airplane Transfer Function for One and Two Degrees of Freedom

30
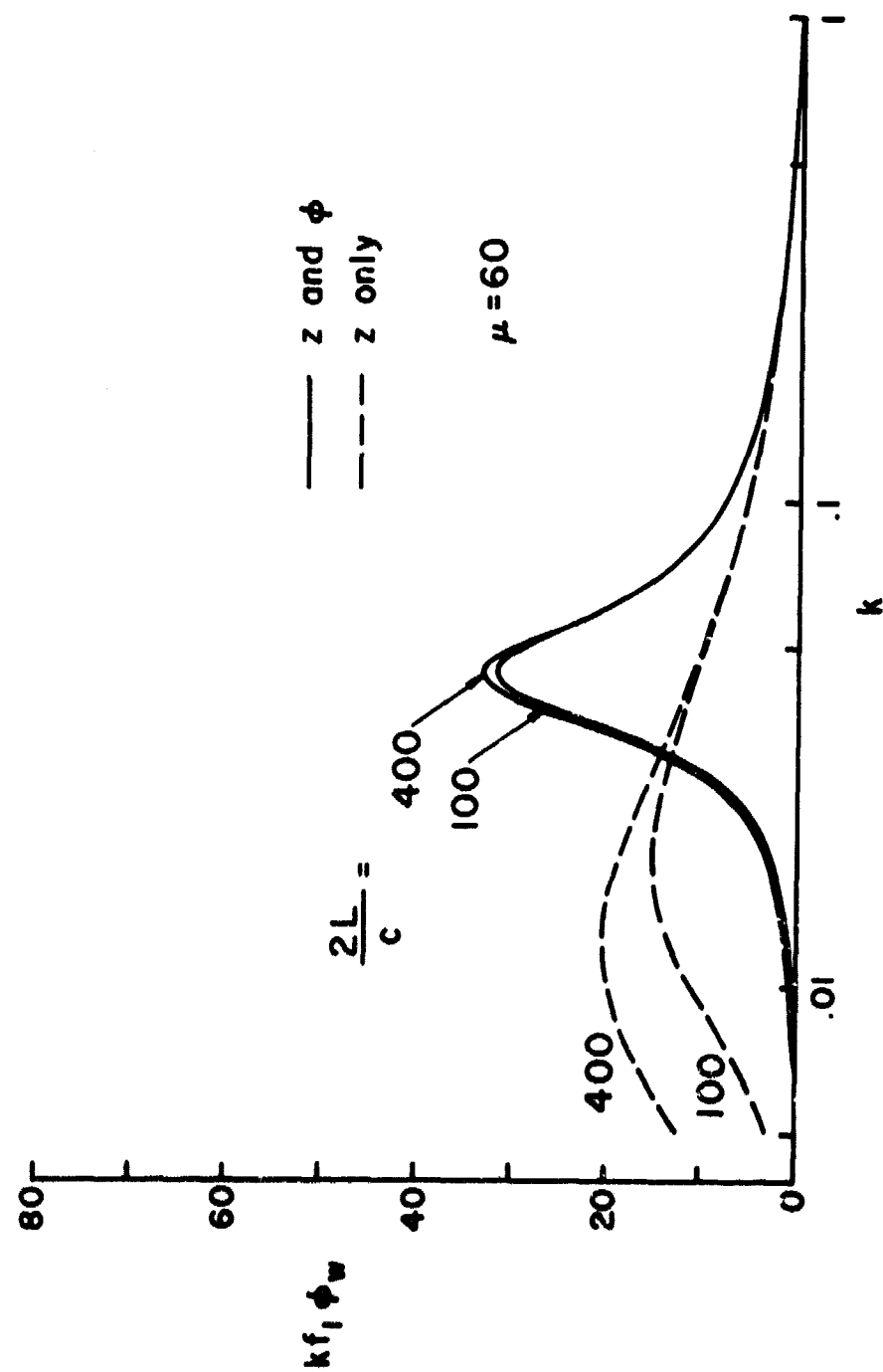
Figure 7.- Distribution of Response Power for One and Two Degrees of Freedom
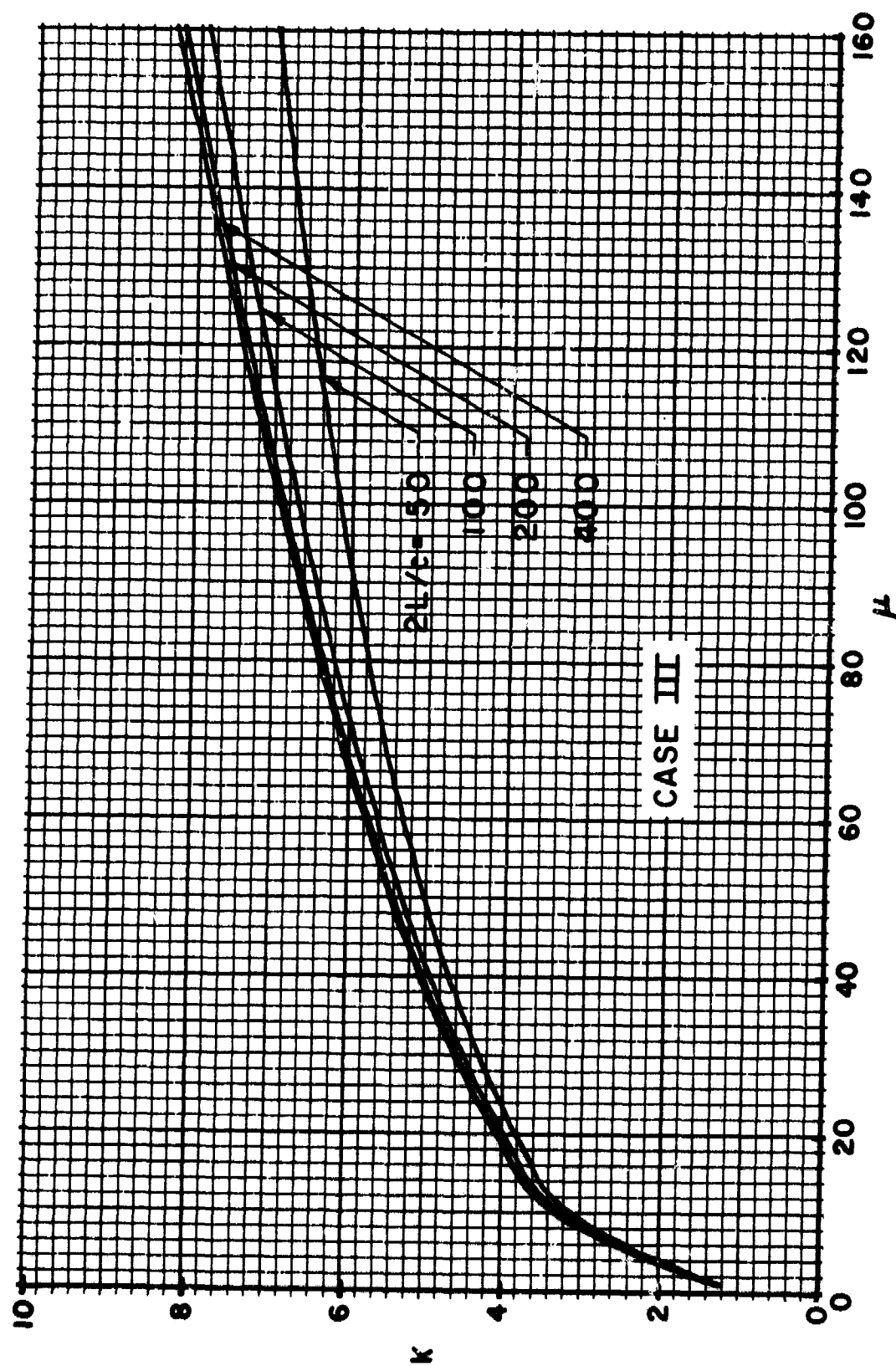
Figure 8.- K Curves for Case III
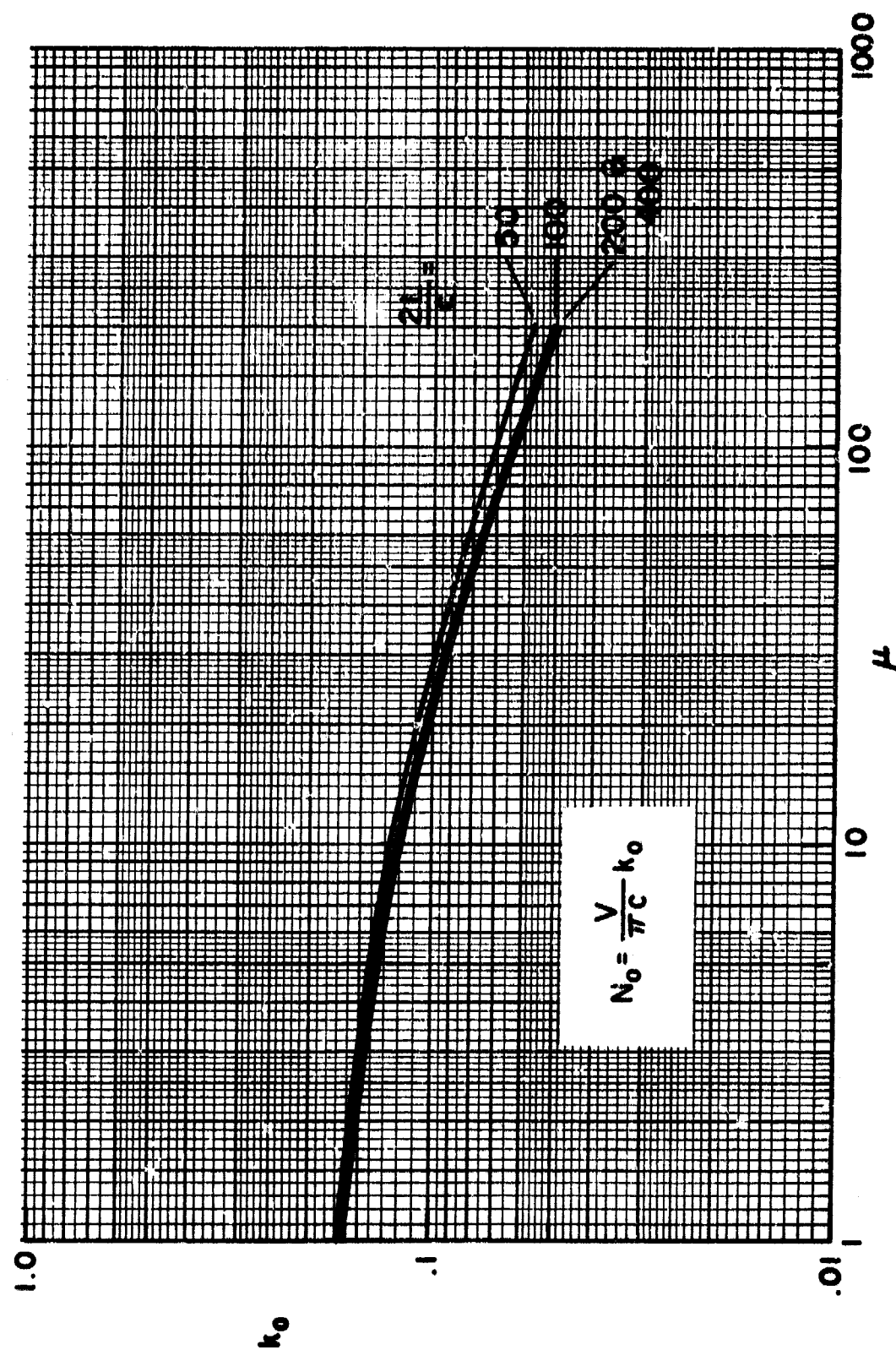
Figure 9.- k_o Curves for Case III

$$N_o = \frac{V}{\pi C} k_o$$

33
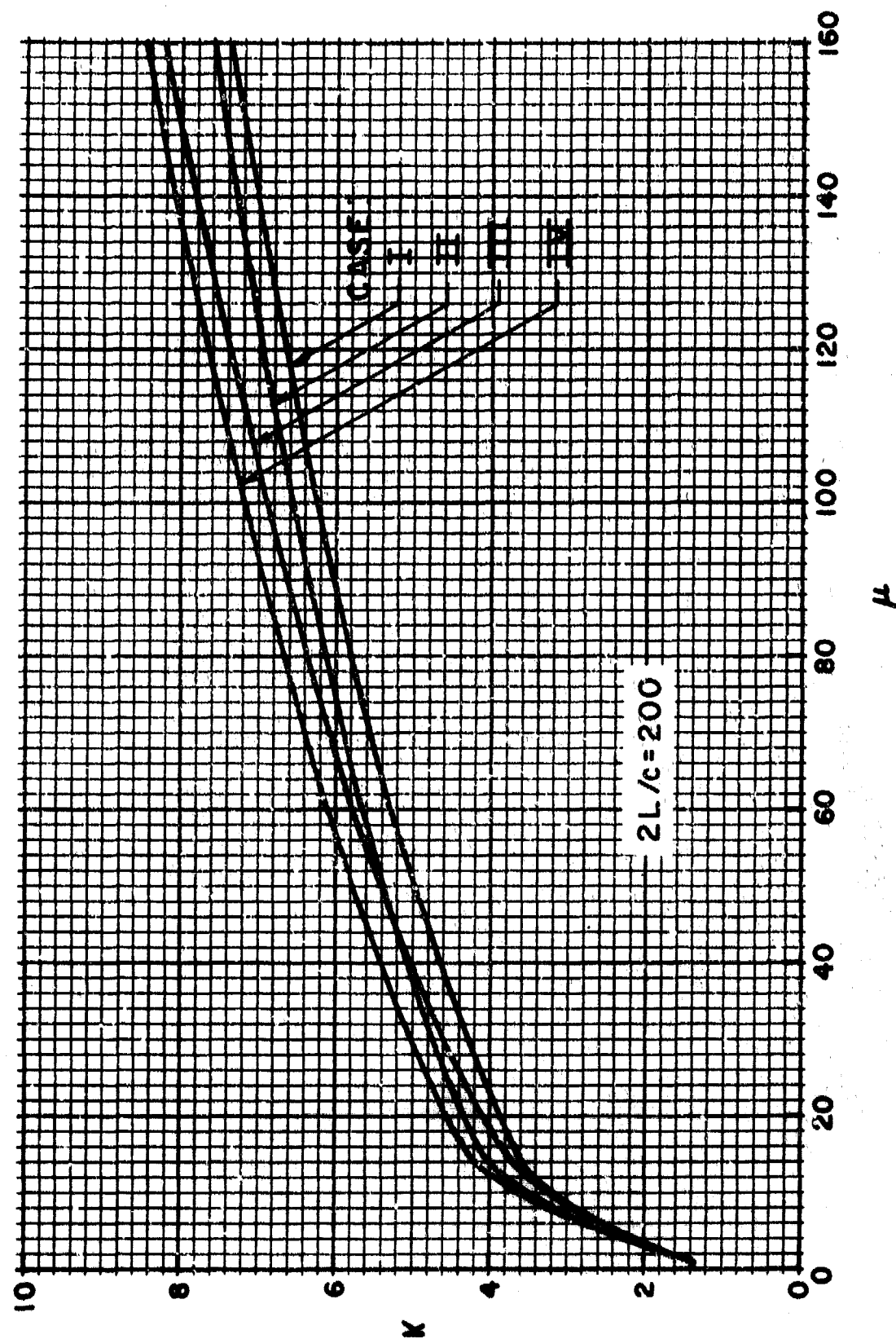
Figure 10.-- K Curves for Cases I, II, III and IV

34
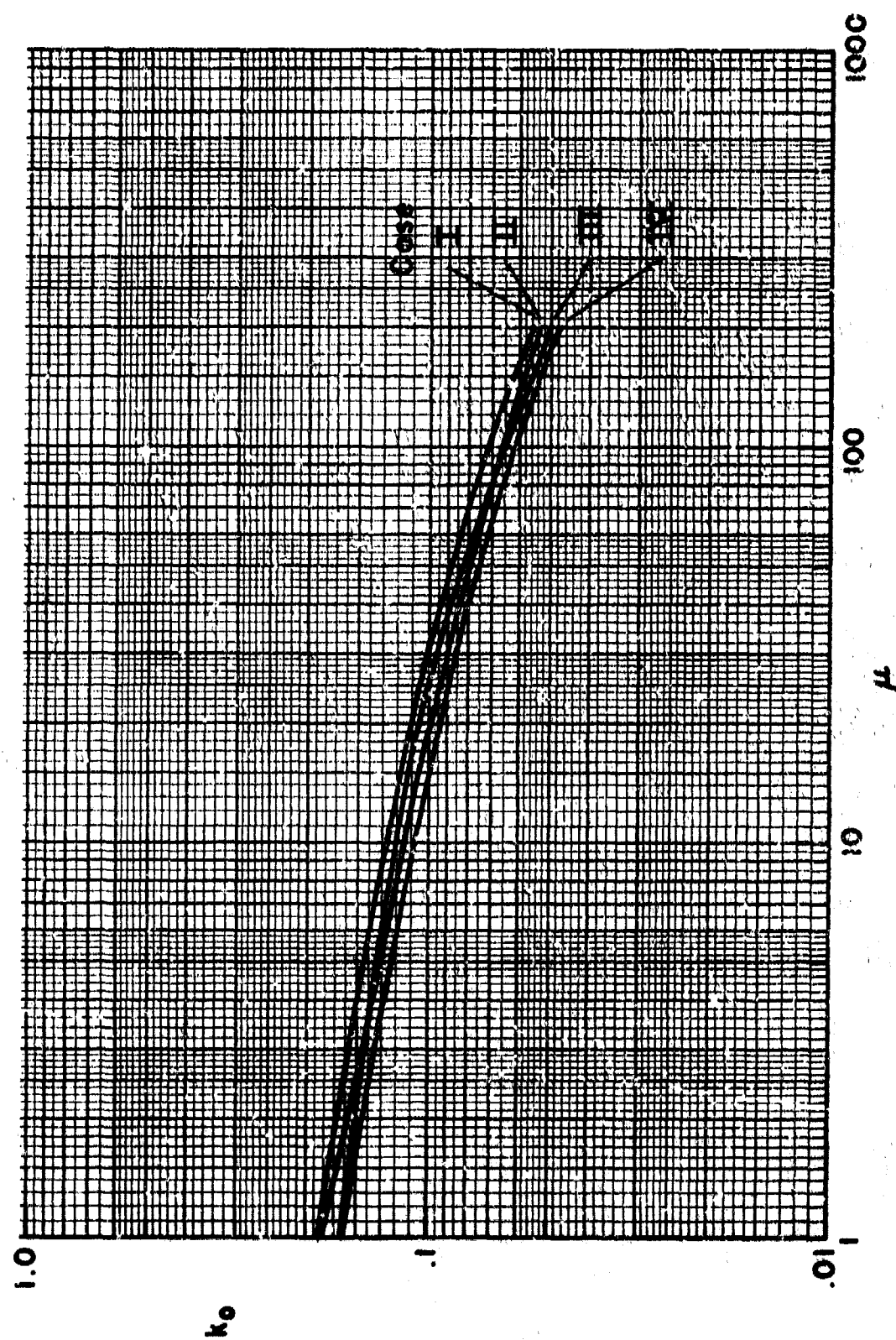
Figure 11.- k_o Curves for Cases I, II, III and IV

35
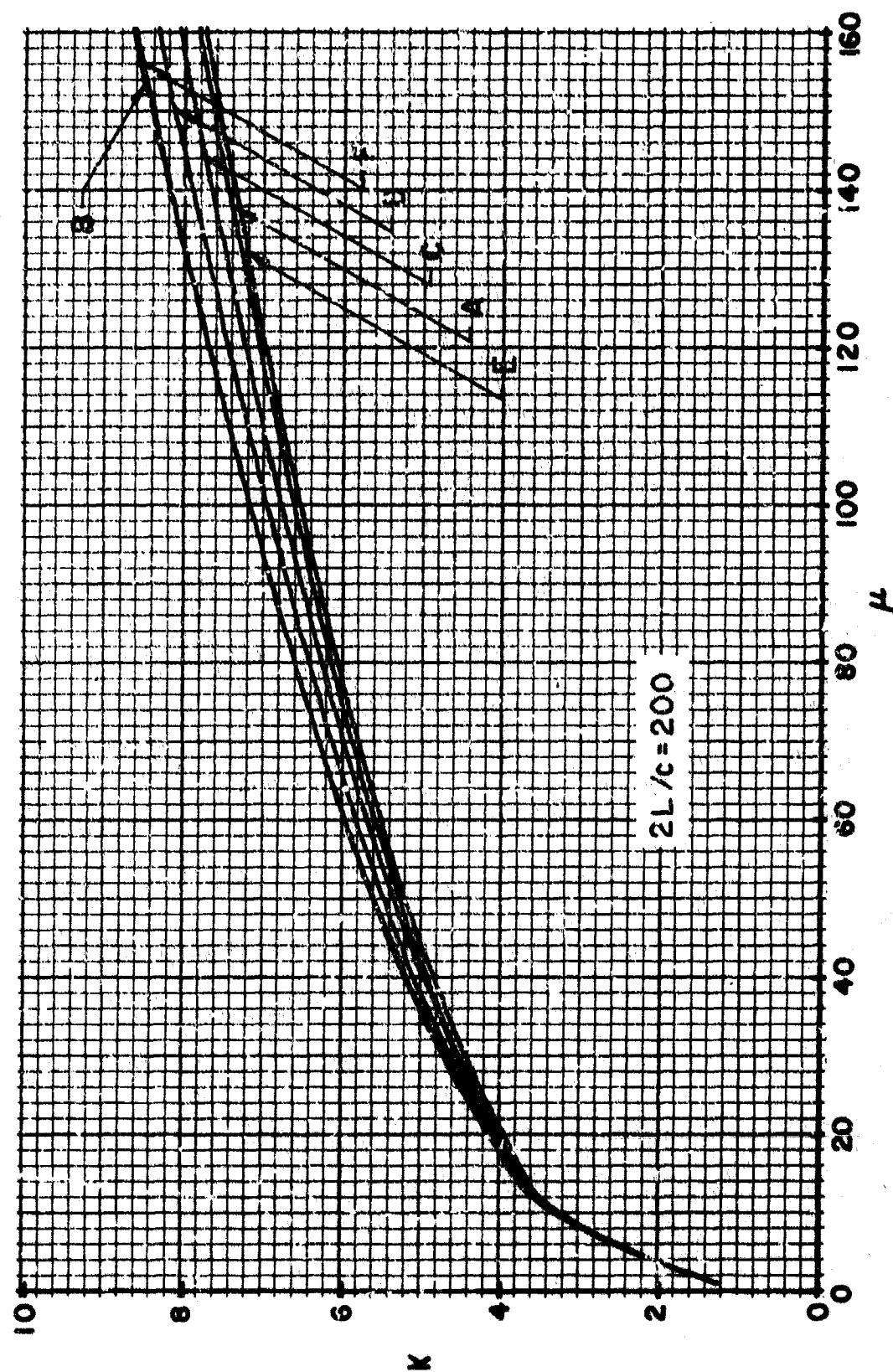
Figure 12.- K Curves for Cases with Parameter Variations
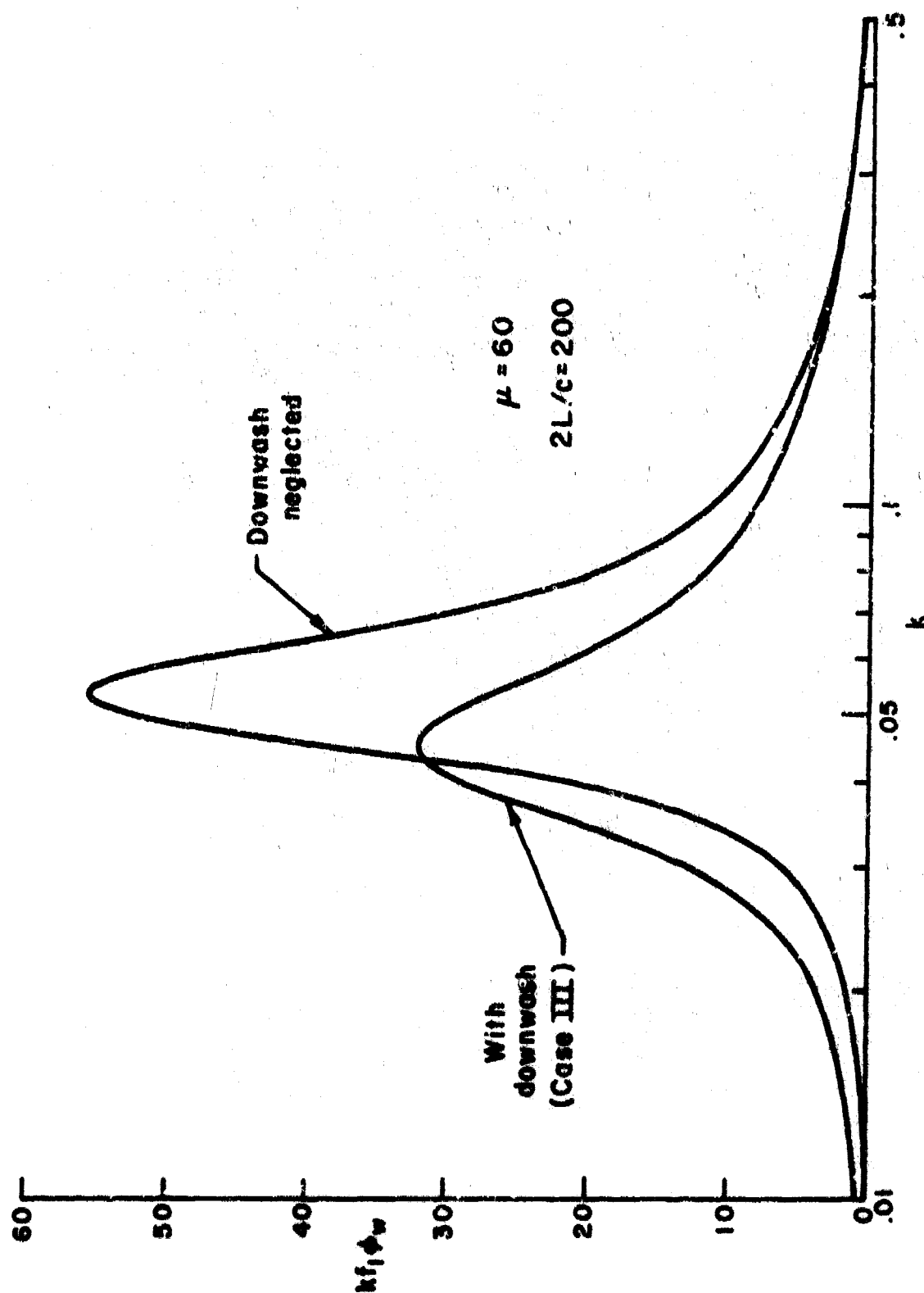
36
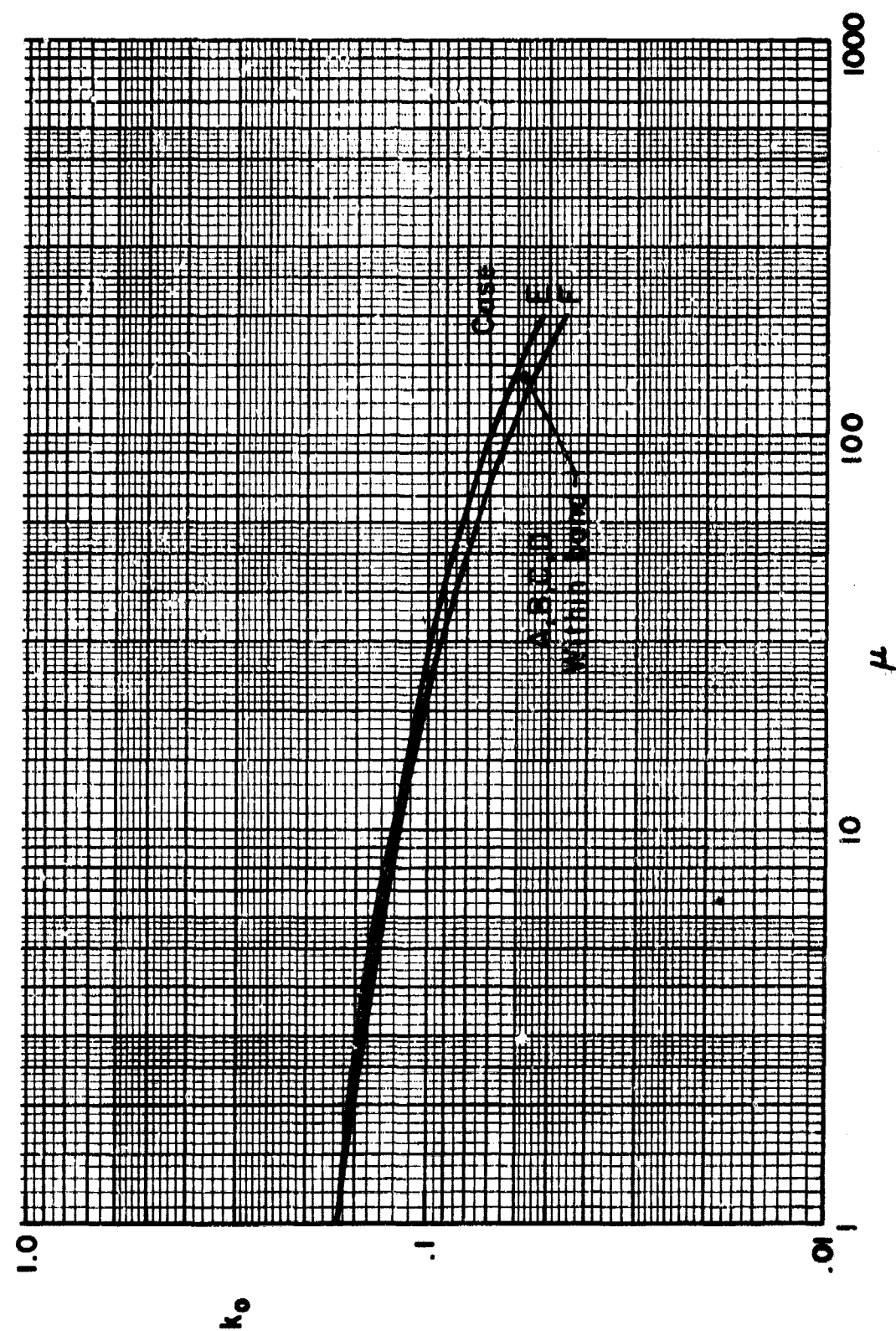
Figure 13.- k_o Curves for Cases with Parameter Variations

37

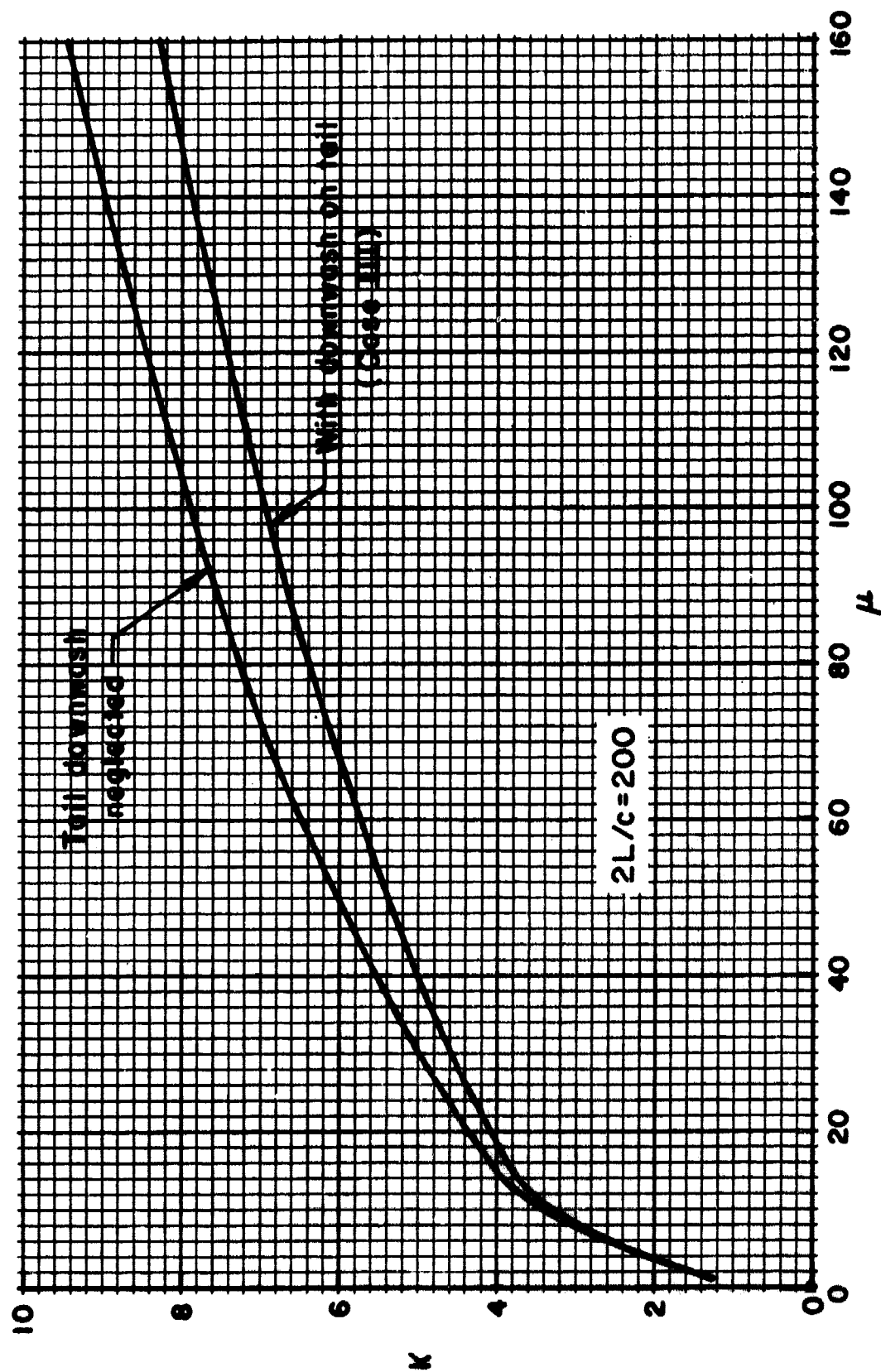Figure 14.- Effect of Tail Downwash on Airplane Transfer Function
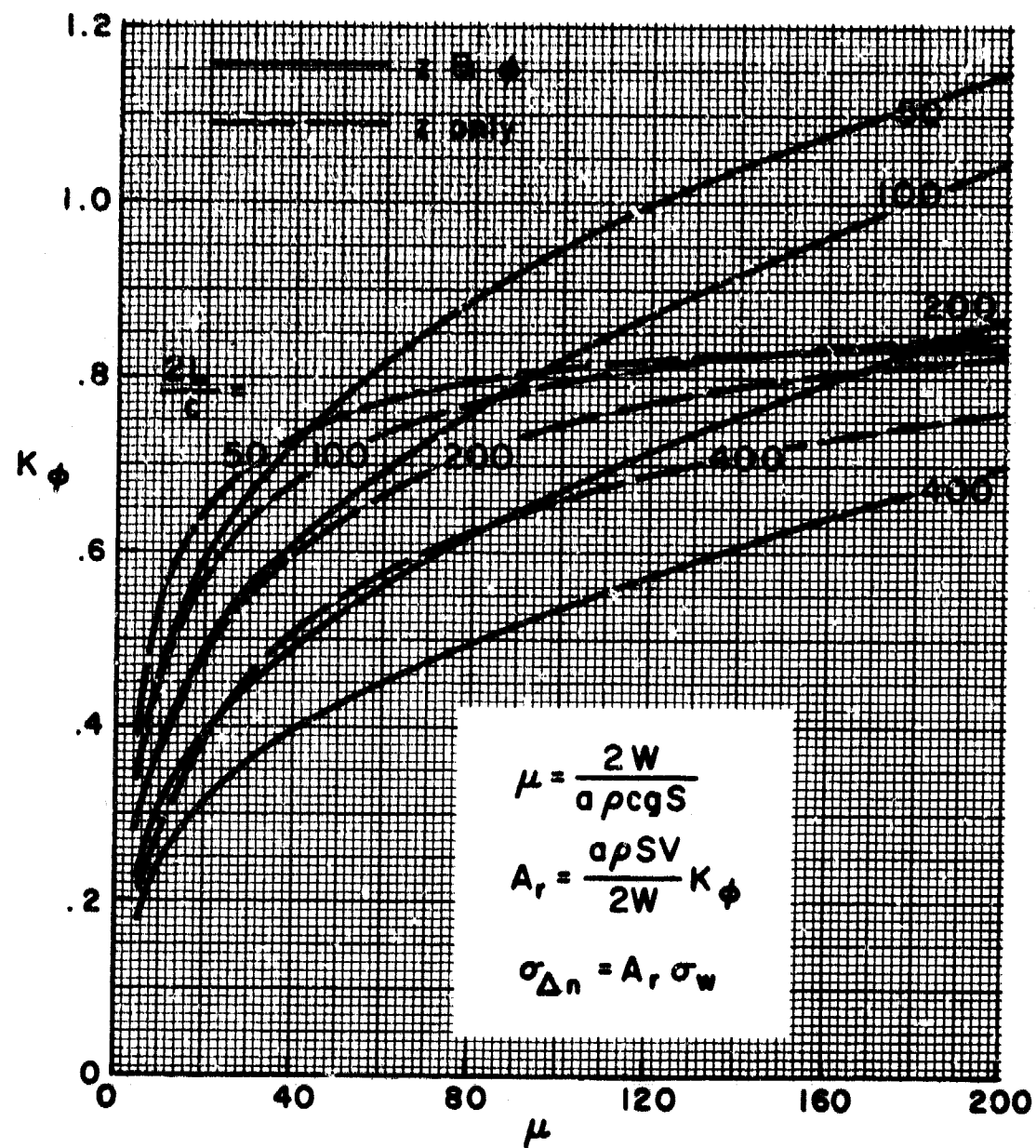
Figure 15.- Effect of Tail Downwash on K Curve

Figure 16.- Comparison of Spectral Alleviation Factor for Airplanes
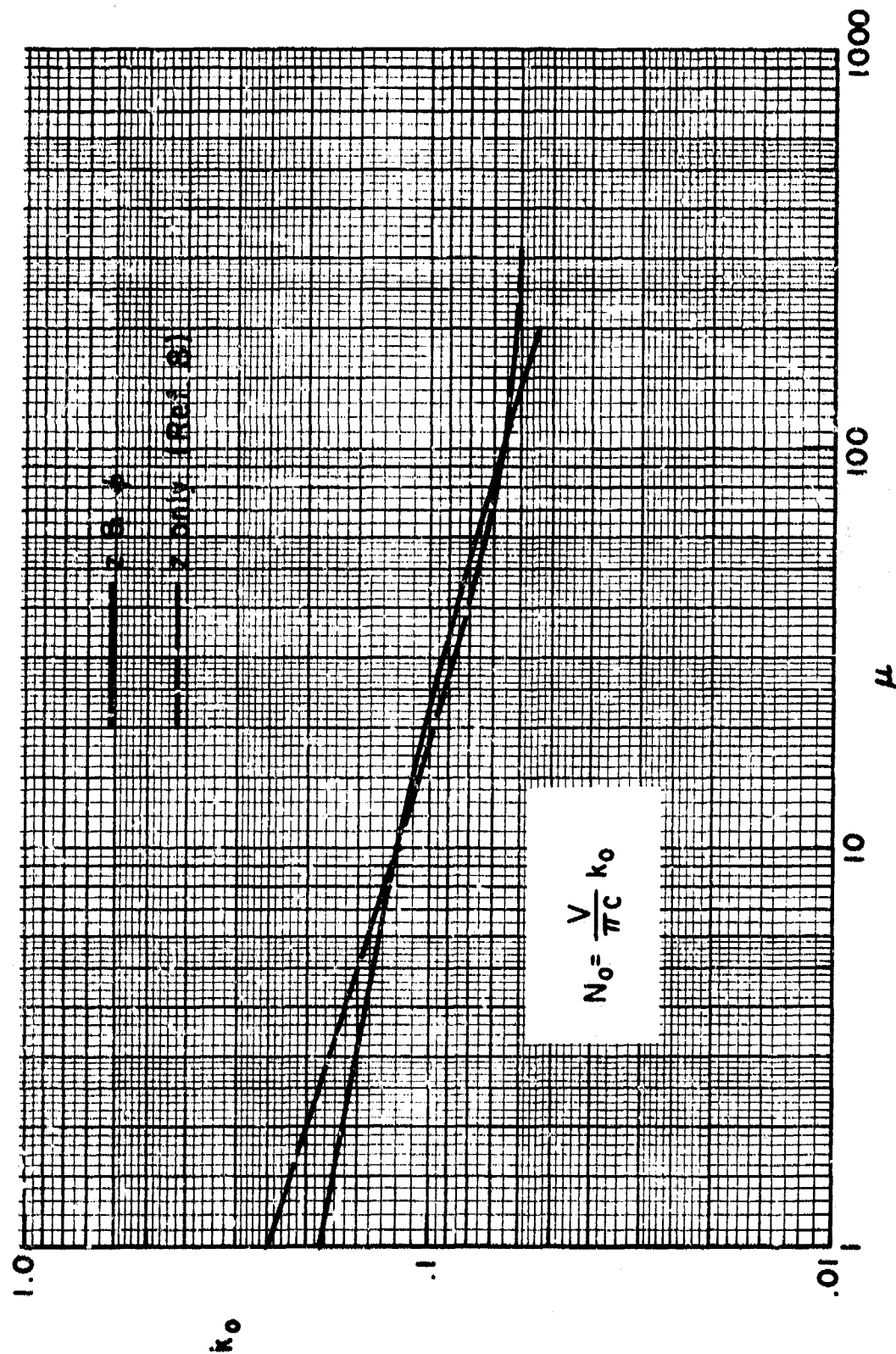with One and Two Degrees of Freedom

Figure 17.- Comparison of k_o Curves for Airplanes with One and Two Degrees of Freedom

41